buildings

MDPI

Article

Assessing Seismic Vulnerability and Structural Resistance in Urban Areas: A Case Study of Demetevler/Yenimahalle in Ankara †

Ramazan Serdar Eser [1] and Şule Bakırcı Er [2,*]

[1] Graduate School of Natural Applied Sciences, Civil Engineering, Kırıkkale University, Kırıkkale 71450, Türkiye; rseser@gmail.com
[2] Department of Civil Engineering, Faculty of Engineering and Natural Sciences, Kırıkkale University, Kırıkkale 71450, Türkiye
* Correspondence: sulebakircier@kku.edu.tr
† This paper is an extended version of This article is a revised and expanded version of a paper entitled "Investigation of Buildings with Rapid Street Survey in Ankara Yenimahalle Demetevler Region" (In Turkish "Ankara Yenimahalle Demetevler Bölgesinde Yapıların Hızlı Sokak Taraması Yöntemiyle Değerlendirilmesi"), which was presented at Internatıonal Korkut Ata Scıentific Researches Conference, Osmaniye Korkut Ata University, 28–30 June 2022, Osmaniye, Türkiye.

Abstract

Driven by Türkiye's high seismicity, rapid vulnerability assessment of existing building stocks is vital for disaster risk reduction. This study evaluates the seismic safety of 536 buildings in the Demetevler, Demetlale, and Demetgül neighborhoods of Ankara's Yenimahalle district using a rapid visual street survey based on structural and architectural risk indicators. Additionally, a single-mode nonlinear pushover analysis was conducted on a representative high-risk building to evaluate element-level damage. The results show that 47% (252 buildings) of the assessed stock are classified as high risk, with vulnerability exceeding 55% for structures with six or more storeys at a risk score of 50. The pushover analysis revealed that 16% of the primary structural elements in the sample building would sustain damage. These findings highlight the urgency of targeted urban renewal and confirm rapid visual screening as an effective decision-support tool for preliminary regional assessment.

Keywords: rapid visual screening; seismic vulnerability; Sucuoğlu–Yazgan method; seismic risk

Check for updates

Academic Editors: Gabriele Milani and Antonio Formisano

Received: 31 August 2026
Revised: 23 October 2026
Accepted: 2 November 2026
Published: 18 November 2026

Copyright: © 2026 by the authors. Licensee MDPI, Basel, Switzerland. This article is an open access article distributed under the terms and conditions of the Creative Commons Attribution (CC BY) license.

1. Introduction

Yenimahalle is a district located in the northwestern part of Ankara. A large portion of the district is situated on terrestrial clastic units belonging to the Pliocene period, while the neighborhoods located in the northern part of the district center are predominantly represented by Miocene-aged units [1]. A geological map of the region is presented in Figure 1.

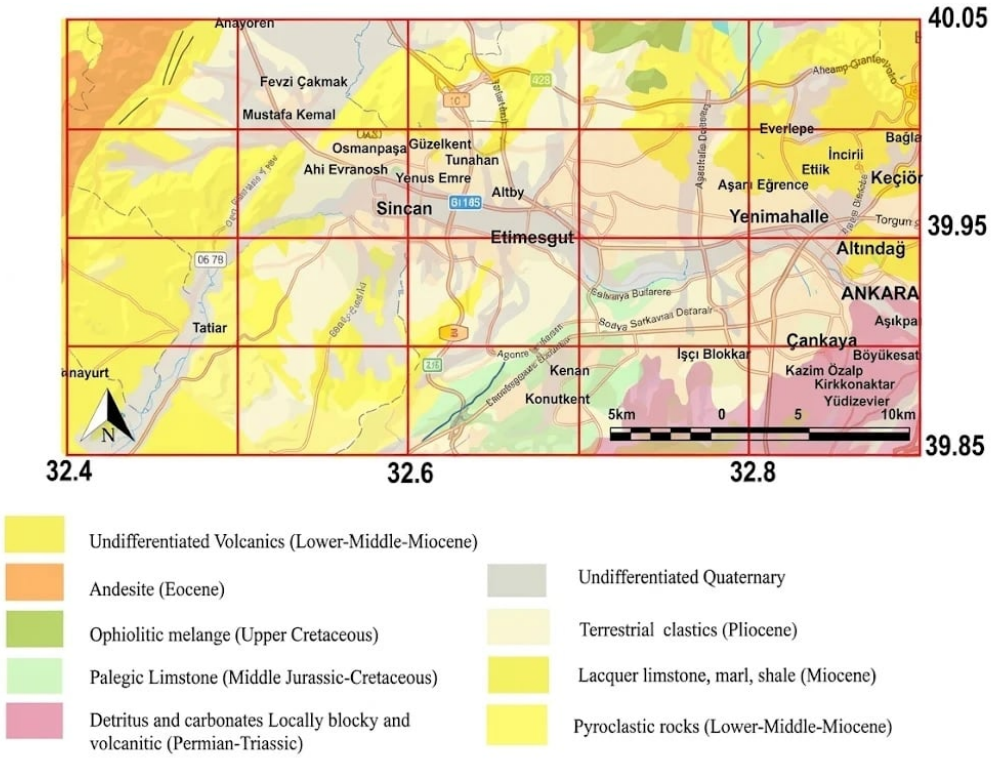


Figure 1. Geological structure of the region [2].

Soil–structure interaction plays a critical role in the design of earthquake-resistant structures. In particular, local soil conditions and the dynamic behavior of subsurface layers significantly influence the seismic forces acting on structures during an earthquake. Among these dynamic properties, the shear wave velocity (Vs) is one of the most important parameters, commonly determined through in situ seismic tests and widely used in assessing the geotechnical characteristics of soils. In Felek's study, the shear wave velocities, site amplification factors, and fundamental vibration periods of Plio-Quaternary units located in the Ankara region were determined and analyzed. Surface-wave-based Vs30 is presented in Figure 2. Comparative evaluations were conducted using microtremor data. Based on the results, site classification, amplification levels, and predominant vibration periods were assessed. Scientific recommendations regarding the geotechnical suitability and potential seismic risks of the investigated units are also presented [3].

Based on the experiences gained from past earthquakes and subsequent scientific research, structural design codes and standards have been continuously updated, and these advancements are implemented in new constructions. However, a substantial portion of the building stock in Türkiye was constructed in accordance with outdated regulations and remains in use today. Considering the country's location along active seismic fault lines, ensuring that structural design and construction practices conform to current seismic codes and contemporary engineering standards is of critical importance.

While assessing each building through its original structural drawings or as-built surveys to determine both linear and nonlinear behavior is the most accurate approach, it is time-consuming and impractical for large-scale applications.

In assessing the seismic safety of existing building stocks, rapid visual screening (RVS) (first-tier) and detailed nonlinear structural analyses (second-tier) function as complementary tiers. While detailed analyses provide element-level structural performance, RVS ensures that limited engineering and financial resources are efficiently prioritized toward high-risk structures. Previous studies have addressed various aspects of seismic vulnerabil-

ity, ranging from local street-level surveys to regional hazards and advanced computational modeling [4–29]. However, significant gaps remain regarding how first-tier screening results directly align with second-tier quantitative damage predictions in specific urban typologies, a gap that this study directly addresses.

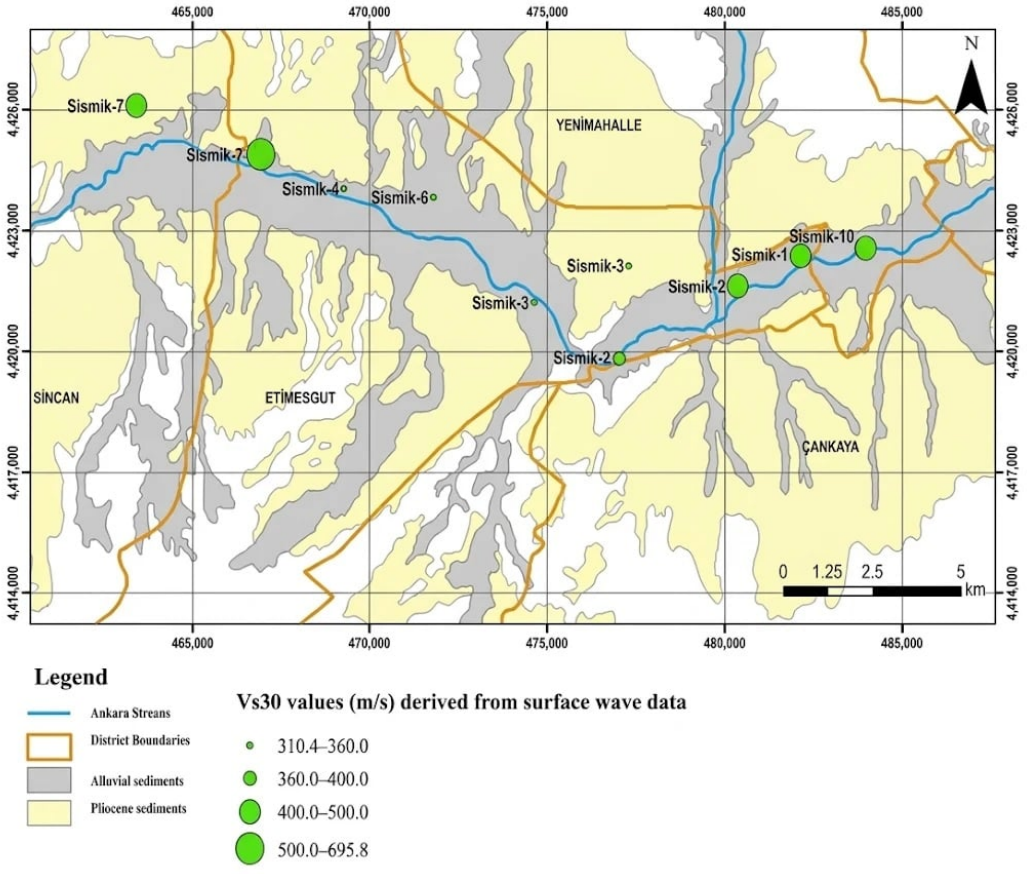


Figure 2. Surface-wave-based Vs30 map [3].

Rapid screening methods have been extensively applied both in Türkiye and globally to evaluate regional vulnerabilities. Foundational local methodologies, such as the street-level survey framework developed by Sucuoğlu et al. [4,7] based on damage data from the 1999 Düzce earthquake, established the statistical basis for first-tier assessments. Subsequent large-scale deployments—such as Yakut et al. [8] screening ~100,000 buildings in Istanbul, Sömezer et al. [9] evaluating 2074 structures in Kırıkkale, and Yeniçelik [10] analyzing northern Çankaya—demonstrated the efficiency of RVS in identifying high-risk regional clusters. Similar applications by Aynur and Meydanlı Atalay [11] in Yalova reaffirmed strong correlations between visual risk parameters (e.g., soft storeys, storey count) and structural damage.

Globally, RVS methodologies have evolved through digital integration and local calibration. International studies have adapted tools like FEMA 154 to local conditions using geospatial platforms (Kassem et al. [13] in Malaysia) or mobile applications (Nanda et al. [14] in India; Rodrigues et al. [29] in Brazil). Others have incorporated soft computing, artificial neural networks, and optimization algorithms to refine RVS accuracy (Harirchian et al. [12]; Bektaş and Brassai [18]; Grover [19]). Moreover, comparative evaluations by Harirchian et al. [26] against the 2003 Bingöl earthquake emphasized that localized screening methods yield far more realistic damage predictions for reinforced concrete stock than generic international codes.

While the aforementioned literature heavily relies on purely statistical screening or macro-level hazard assessments (e.g., Mulwa [20]; Zymvragakis et al. [21]; Hamdache et al. [22]), a crucial limitation persists: First-tier screening alone lacks element-level structural validation. Recent advancements have attempted to bridge this gap using machine learning, hybrid CNN-LSTM models, or tree-based ensemble algorithms to predict structural capacities and damage factors (Yan et al. [24]; Chen [25]; Bıçakçı et al. [27]). However, these data-driven models require massive training datasets and often lack direct physical mechanics.

Fewer studies have directly cross-validated qualitative RVS scores against deterministic physical analyses. For instance, Purushothama and Monteiro [16] demonstrated that while RVS is highly useful for initial screening, numerical validation via nonlinear modeling remains essential to define true safety margins. Similarly, probabilistic and reliability-based structural evaluations (Salim et al. [23]; Rodrigues et al. [28]) highlight the necessity of detailed structural demand analysis for high-risk buildings.

Unlike previous regional studies that either limit their scope strictly to first-tier street surveys (e.g., [8–10]) or focus purely on complex regional seismicity/machine learning without field-level screening (e.g., [21,24,27]), this study provides an integrated two-tier evaluation framework. By focusing on the mid-rise residential building stock of Ankara's Demetevler district—a high-density urban area with well-documented construction deficiencies—this research not only establishes a comprehensive first-tier risk profile across 536 buildings using the Sucuoğlu and Yazgan method [4] but also directly complements and validates these screening scores by performing a second-tier nonlinear single-mode pushover analysis on a representative high-risk building. This dual approach effectively links observational street-level indicators with quantitative plastic hinge formation, thereby delineating the operational limits and safety margins of first-tier rapid assessments.

Local authorities are implementing urban renewal projects, taking into account the seismicity of Türkiye. A significant portion of the existing building stock was constructed decades ago, often without taking into account codes and technological materials and practices. The seismic resilience of these buildings remains uncertain, causing concern among residents. It is important to identify the seismic risk of these old buildings in order to take necessary retrofitting measures and ensure their continued safe use.

In Yenimahalle, an urban development project involving approximately 5000 housing units was carried out over a period of 3 to 5 years, facilitated by low-cost land and favorable credit policies in the 1950s [30].

The region is affected by nearby fault zones. The epicenter of the earthquake that occurred on 25 August 2019 was located within the Yenimahalle district and was felt across the central districts [1].

The present study focuses on the assessment of building's fragility prior to conducting a detailed structural analysis in Yenimahalle, Ankara, which is the initial phase of the process. The methodology (Rapid Street Survey Assessment Method) was developed by Sucuoğlu and Yazgan [4] for the purpose of evaluating existing buildings through external observation during field research. In order to calculate a general risk rating for a building, a variety of structural and architectural parameters are taken into consideration. Subsequently, the risk level is determined in accordance with this value.

The risk indicators derived from this study will assist in establishing a priority ranking for urban renewal projects and detailed structural evaluations within the region. Additionally, this work will enhance awareness of urban transformation practices and pave the way for the broader implementation of similar studies.

To address the gaps, this study establishes both practical and scientific objectives. The practical goal is to outline the urgent seismic risk profile of the densely populated

building stock in the Demetevler, Demetlale, and Demetgül neighborhoods of Ankara's Yenimahalle district, thereby supporting municipal urban renewal and mitigation planning. The scientific goal focuses on investigating the correlation, validation limits, and predictive consistency between rapid visual street screening (RVS) results and detailed nonlinear single-mode pushover analysis.

Based on these objectives, this study addresses two core research questions and their corresponding hypotheses. First, it investigates the extent to which rapid visual street survey risk classifications align with structural damage states predicted by nonlinear pushover analysis, hypothesizing that rapid visual screening reliably identifies high-risk structures while exhibiting conservative safety thresholds that can be effectively cross-validated through element-level pushover assessments. Second, it examines how vertical irregularities and building height (e.g., storeys ≥ 6) proportionally amplify seismic vulnerability in this specific urban typology, positing that structures exceeding six storeys combined with vertical irregularities experience a disproportionate escalation in overall vulnerability rates.

2. Materials and Methods

In this study, a preliminary seismic risk assessment of structures was conducted using the rapid street survey method. Evaluating the seismic risk of existing buildings in the face of potential earthquakes is critical for implementing necessary mitigation measures in advance. An overview of Türkiye's seismicity and common rapid structural assessment techniques is presented, alongside the specific assessment methodology developed by Sucuoğlu and Yazgan that was adopted in this study.

2.1. Earthquakes and Their Effects in Turkiye

Earthquakes are widely considered to be one of the most common and destructive natural disasters worldwide. They are triggered by movements of the Earth's tectonic plates, and their effects vary depending on the geographical location, size, and focus depth. Major seismic events can cause serious ground cracking, landslides, structural collapse, and tsunamis. In addition to their physical effects, earthquakes can have deep socio-economic consequences, including infrastructure damage, economic loss, and significant public health issues.

Turkiye is located in a seismically active region and intersects with several major fault lines, including the North Anatolian Fault (NAF), the East Anatolian Fault (EAF), and the Mediterranean Fault Zone. Consequently, earthquake preparedness and urban planning strategies are of great importance in our country, where earthquakes occur frequently.

Alongside structures built in accordance with specifications and regulations in our country, there are also buildings constructed without taking earthquake regulations into consideration and without receiving engineering services. Structural damage vulnerability is being prevented/reduced through urban renewal projects of local governments.

The destructive consequences of seismic events in Turkiye underscore the necessity of conducting ongoing research, employing data-driven risk assessment methodologies, and implementing effective mitigation strategies. For instance, the 7.7 and 7.6 magnitude earthquakes that occurred in Kahramanmaraş in February 2023 were among the most significant natural disasters in the country's history. These earthquakes had a widespread impact, affecting 11 provinces and resulting in the loss of over 50,000 lives and significant structural damage. Another significant event was the 1999 Izmit (Marmara) earthquake, which had a magnitude of 7.4 and caused widespread destruction across northwestern Türkiye, resulting in thousands of deaths and significant damage to infrastructure. In a similar manner, the 2011 Van earthquake (7.2 magnitude) resulted in extensive structural damage across eastern Anatolia.

The seismic events in question have not only resulted in a tragic loss of life but have also incurred economic damages amounting to billions of Turkish Lira. This underscores the urgent need for proactive seismic resilience planning.

As illustrated in Table 1, significant seismic events and their subsequent impacts are presented.

Table 1. Major earthquakes in Turkiye and associated casualties.

Date	Magnitude	Location	Consequences
6 February 2023	Mw 7.7 & 7.6	Pazarcık–Elbistan	Over 50,000 fatalities; 387,346 damaged buildings
17 August 1999	Mw 7.4	Marmara Region	17,480 fatalities; 73,342 damaged buildings
23 October 2011	Mw 7.2	Van	644 fatalities; 17,005 damaged buildings
24 November 1976	Mw 7.5	Muradiye (Van)	3840 fatalities; 9232 damaged buildings

As demonstrated in Table 1, the occurrence of such substantial seismic events in Türkiye underscores the paramount importance of ensuring the seismic resilience of buildings. It is imperative to undertake a thorough evaluation of the seismic vulnerability of existing building stock. However, the process of determining the seismic performance of a single building is time-consuming, and the evaluation of the entire building stock will require a significant amount of time and labour.

In order to address this issue, the Turkish government enacted Law 6306 on the Transformation of Areas under Disaster Risk, which was published on 16 May 2012. The legislation encompasses provisions for the identification of "risky buildings" [31]. In accordance with the provisions of the aforementioned legislation, buildings may be subject to rapid seismic assessment procedures as a preliminary step to facilitate the prioritization of detailed structural assessments. The provisions outlined herein facilitate the effective screening of vulnerable structures without the necessity for full-scale analyses at the preliminary stage.

The district of Yenimahalle, which is the subject of this study, is located within the administrative boundaries of Ankara, the capital city of Turkiye. The major tectonic structures affecting Ankara and its surrounding area are shown in Figure 3.

2.2. Rapid Structural Assessment Methods

The methods used for rapid assessment of buildings are summarized below.

2.2.1. USA RVS Method (FEMA P-154)

This method is principally employed in the context of rapidly assessing seismic vulnerability in regions characterized by a high propensity for seismic activity. The evaluation process involves a visual assessment by an external (and potentially internal) assessor, who records their observations on a standard form. The calculation of the performance rating is based on the following parameters: the structural system type, the construction year, the soil type, the seismic zone, the plan and vertical irregularities, the adjacent buildings, geological hazards, and the status of non-structural components. In the context of the construction industry, assessments are to be conducted in accordance with the prevailing seismic regulations that are in effect at the time.

2.2.2. Canadian Seismic Screening Method

This method involves the collection of observational data through the utilization of a data collection form, encompassing both structural and non-structural components. The Structural Index (SI) and the Non-Structural Index (NSI) are computed, and the resulting values are summed to obtain a performance score. The significance of the structure is also taken into account. The allocation of buildings to categories is determined by the score

obtained, with buildings being classified as low, medium, or high priority or very hazardous based on the score.

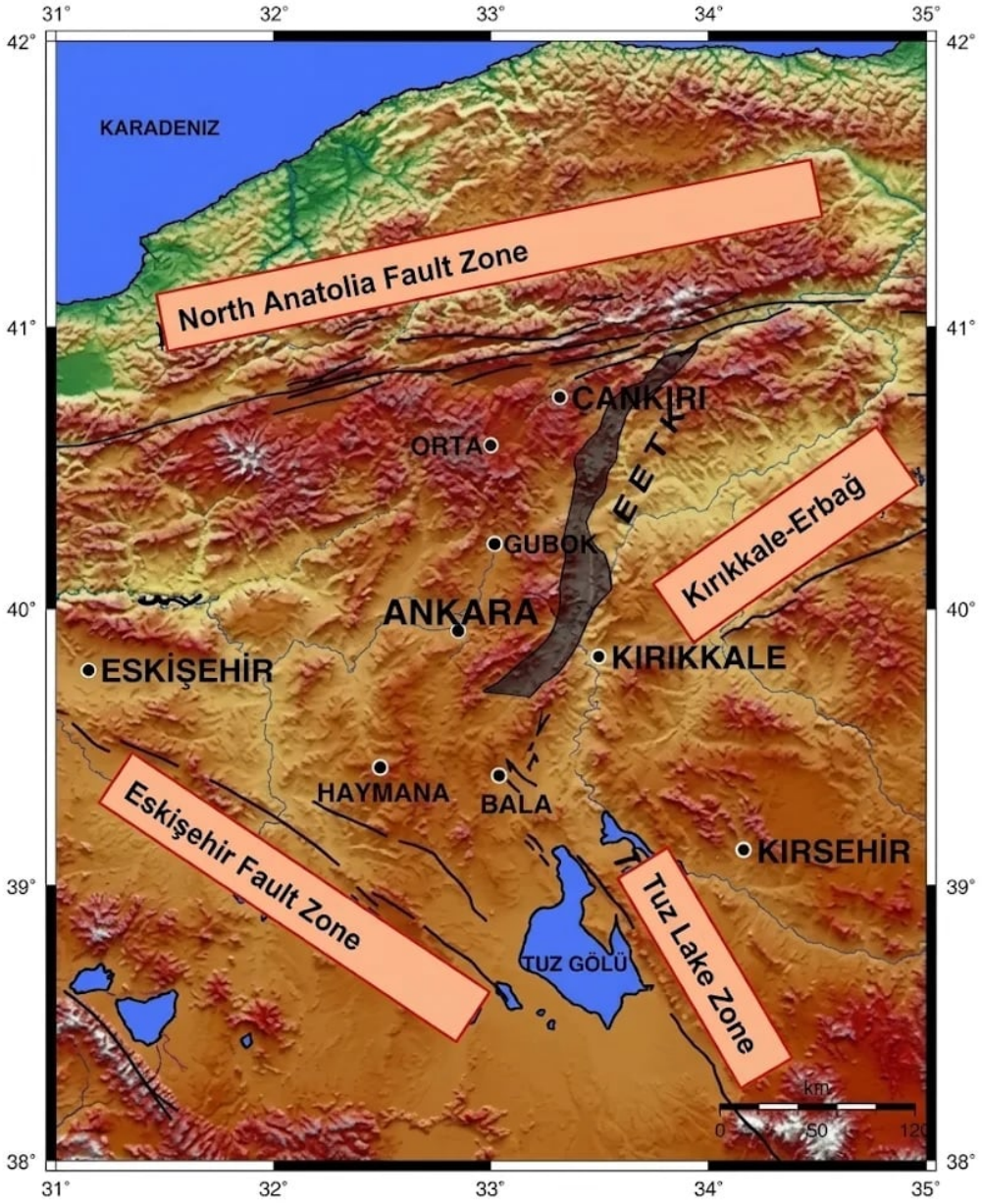


Figure 3. The major tectonic structures affecting Ankara [3].

2.2.3. Indian RVS Method

This methodology, which has been adapted from FEMA P-154 to align with Indian conditions, employs a rating system predicated on specific parameters. These include building height (mid/high-rise), vertical and plan irregularities, compliance with the grid, and soil type. The objective of the process is to obtain a final score representing the building's seismic vulnerability. This is achieved by aggregating all the parameters.

2.2.4. Sucuoğlu Method (Türkiye)

In this method, the buildings are evaluated and ranked according to their seismic risk by utilizing observable parameters from the street. The initial performance scores are adjusted using various structural quality factors, including visible structural elements and seismic hazard zones. Further considerations include the height of the building and the

year of construction. The classification of buildings as high risk or low risk is typically accomplished through the utilization of a cut-off point (e.g., Risk Score (RS) = 50).

2.3. Method

The Sucuoğlu and Yazgan method is a rapid visual screening approach that is based on observations at street level and is used to evaluate the seismic vulnerability of buildings. The method was developed through the analysis of damaged or collapsed reinforced concrete buildings during the 1999 Düzce earthquake in Türkiye, using statistical correlations based on their physical characteristics. Although internationally recognized frameworks like FEMA 154 exist, the Sucuoğlu and Yazgan method was selected for this study due to its specific calibration to the unique traits of the Turkish building stock. Its rapid execution and regional adaptability make it an ideal assessment tool for the surveyed district. Nevertheless, subjective judgments among evaluators can introduce minor variations in final risk score calculations. The method under scrutiny is designed to evaluate a range of structural and non-structural parameters that contribute to the attainment of performance scores. A lower score is indicative of a higher seismic risk. The following parameters have been utilized in the experimental procedure. Figures in this part were derived from site field observations.

2.3.1. Total Number of Floors

A direct relationship is observed between the number of floors and earthquake magnitude. When buildings are designed and constructed without engineering services and do not have sufficient lateral rigidity, the ratio of damage increases. Determination of floor numbers is shown in Figure 4.



Figure 4. Sample building and determining the number of floors.

2.3.2. Soft/Weak Storey

Soft floors are usually formed at ground levels, typically due to the absence of storefront glazing and infill walls that reduce stiffness. Taller ground floors create uneven displacements, increasing seismic vulnerability. This is common in mixed-use buildings with shops at street level and residential above. A soft storey is shown in Figure 5.



Figure 5. Sample soft storey image.

2.3.3. Heavy Overhangs

Cantilevers above the entry level induce mass and stiffness irregularities. These overhangs often cause discontinuities in structural elements and increase damage during earthquakes. These applications are common in many structures. Heavy overhangs are illustrated in Figure 6.



Figure 6. Heavy overhangs in two facades of a building.

2.3.4. Short Columns

Short columns are typically formed in basements due to partial wall infill or small windows. These elements experience higher shear forces, leading to severe damage. This phenomenon is commonly observed in basement-level columns with strip windows. There is a short-column example in Figure 7.



Figure 7. Short-column effect in strip windows.

2.3.5. Visible Structural Quality

Poor workmanship and material quality (e.g., low concrete strength, inadequate reinforcement) increase seismic risk. Indicators include honeycombing in concrete, improper reinforcement placement, and structural voids during concrete casting. Figure 8 gives an idea of the quality of a building.



Figure 8. Representative view of a building with poor construction quality.

2.3.6. Pounding Effect

Inadequate separation between adjacent buildings with different floor heights can lead to pounding during seismic events. This often results in floor misalignments and inter-building collisions, particularly in densely built-up areas. Buildings with different floor levels are shown in Figure 9.



Figure 9. Adjacent buildings with incompatible floor levels (pounding effect).

2.3.7. Topographic Effect

Buildings on steep slopes are more prone to differential settlement and seismic damage due to uneven load distribution from foundations to superstructures, as confirmed by studies from Sucuoğlu and Yazgan. In Figure 10, a structure on sloping ground is shown.



Figure 10. Example of a structure sitting on sloping ground.

2.3.8. Local Soil Conditions

Soil characteristics play a critical role in seismic damage. Ground motion parameters such as Peak Ground Acceleration (PGA) and especially Peak Ground Velocity (PGV) are used to assess seismic risk. A PGV-based scoring system was developed by Sucuoğlu and Yazgan. For instance, the PGV value for the Demetevler region, according to the Earthquake Hazard Map of Türkiye, is 10.3 cm/s (for 10% exceedance probability in 50 years). PGV values of the Demetevler region are given in Figure 11.



Figure 11. Demetevler region PGV values [32].

2.3.9. Field Forms and Evaluation

Field surveys are conducted via street-level visual inspection using standardized scoring forms. Building features are recorded and photographed to document key risk indicators. These data are then used in desktop analyses to finalize the seismic performance score. The buildings examined via the rapid street screening method in this study were inspected under the observation and supervision of a civil engineer with approximately 20 years of project and application experience, who is also a master's 's student. Prior to the field study, the parameters to be evaluated, their corresponding risk scores, and calculation procedures were thoroughly examined. The average inspection duration for a single building was approximately 10 to 15 min, with observations conducted on weekends. The inspection of all buildings took about 6 months. During the evaluations, parameters such as address information, number of storeys, heavy overhangs, and short-column effects for each building were recorded on the form presented in Figure 12. Subsequently, the risk status of the structure was calculated based on the information compiled in these forms.

Field observations are recorded on standardized forms during on-site surveys. These forms are later digitized during office work and transferred into tables, and all performance scores are calculated.

The score calculation table is shown in Table 2. The total seismic performance score for a building is calculated using the following equation (Equation (1)) developed by Sucuoğlu and Yazgan [4]:

$$\text{Total Score} = \text{PGV-Based Ground Score} - \Sigma\,(\text{Criterion Score} \times \text{Penalty Factor}). \quad (1)$$

In the evaluation process, the penalty score is determined by multiplying the vulnerability parameter by a weighting coefficient of 1 if the parameter is present or 0 if it is absent, which is then deducted from the initial baseline score. Regarding the structural quality assessment, coefficients of 0, 1, and 2 are assigned to good, moderate, and poor quality levels, respectively, and the corresponding penalty points are subtracted from the baseline score.

RAPID SEISMIC ASSESMENT FORM				
SECTION I : BUILDING IDENTIFICATION				
Street :				
Number Of Residental Unit :				
Map Section/Block No/Parcel No:				
City Information System No :				
Construction Year :				
Geographical Coordinates (Lat/Long):				
SECTION II: BUILDING DESCRIPTION				
Number of Stories (Except for basement)				
Embedded Basement	☐ Yes			
Free Story	Number of ☐			
Corrosion	☐ Yes	☐ No	☐ Unobserved	
Approx Width of Front Garden	☐ meters			
Approx Building Front Side Depth	☐ meters			
Heavy Overhangs	☐ Yes			
Building Order	☐ Seperate	☐ Contiguous	☐ Corner Contiguous	
Weak/Soft Story	☐ Yes		☐ No	
Short Column	☐ Yes		☐ No	
Columns at Cantilever Beam	☐ Yes		☐ No	
Height Difference Between Contiguous Buildings	☐ Yes		☐ No	
Slab Levels Between Contiguous Buildings	☐ Yes		☐ No	
Roof Geometry	☐ Gamble	☐ Terrace	☐ Hip	
Observed Building Quality	☐ Good	☐ Moderate	☐ Poor	
Construction Area Slope	☐ No	☐ Low	☐ Steep	
Near to Historical Buildings	☐ Yes		☐ No	
SECTION III: *PLANNING INFORMATION*				
Occupancy	☐ Dwelling	☐ Commercial	☐ Industrial	☐ Public
Ground Story				
Clerestory				
Normal Story				
	Front Garden		**Back Garden**	
Neighborhood Occupancy	☐ Yes	☐ No	☐ Yes	☐ No
Fire Escape	☐ Yes	☐ No		
Lift	☐ Yes	☐ No		

Figure 12. Field observation forms [33,34].

Table 2. Initial and vulnerability parameter scores used in structural risk assessment.

STOREY	VRI 60 < PGV < 80	VRII 40 < PGV < 60	VRIII 20 < PGV < 40	SS	HO	VQ	SC	PE	TE
1	90	125	160	0	−5	−5	−5	0	0
2	90	125	160	0	−5	−5	−5	0	0
3	90	125	160	−10	−10	−10	−5	−2	0
4	80	100	130	−15	−10	−10	−5	−3	−2
5	80	90	115	−15	−15	−15	−5	−3	−2
6	70	80	95	−20	−15	−15	−5	−3	−2
7	70	80	95	−20	−15	−15	−5	−3	−2

VR: vulnerability region. HO: heavy overhang. PGV: peak ground velocity (cm/s). VQ: visual quality. SS: soft storey. SC: short column. TE: topographic effect. PE: pounding effect. The PGV value of 10.3 cm/s obtained from the site-specific field study falls below the lower bound of the lowest discrete evaluation bracket. Alluvial deposits and lacustrine sediments originating from the Ankara Stream form a thick and loose soil layer in the Demetevler region. Therefore, a PGV component of, for example, 10 cm/s in a rock medium has the potential to easily jump into the 20–40 cm/s band within an alluvial column of this scale. Consequently, to maintain analytical continuity and prevent underestimation within the rapid assessment framework, parameters corresponding to the minimum available category (20 < PGV < 40) were assigned.

2.3.10. Yenimahalle–Demetevler Neighborhood

Yenimahalle is one of the largest districts of Ankara Province, Turkiye. Its development began between 1946 and 1949 as part of Ankara's urban planning initiatives. The area was designated by the municipality as a nearby residential area intended to provide housing for low-income workers and civil servants. Yenimahalle officially gained district status on 1 September 1957. Since then, it has become one of the largest and fastest-growing districts of Ankara.

The Demetevler neighborhood, part of the Yenimahalle district, has been identified as a high-risk area in terms of seismic vulnerability due to poor construction quality and adverse geotechnical conditions. The subsoil characteristics and structural deficiencies of buildings in this region significantly increase their susceptibility to potential earthquake damage.

The area included the Demetevler, Demetlale, Demetgül, and Demet neighborhoods, originally developed to meet the housing needs of low-income residents. Strict regulations were applied during early construction phases—for example, buildings had to be completed within one year of starting. Considering the construction technology of that era and these constraints, it is likely that many structures were built with substandard quality.

During the 1960s, due to insufficient supervision of licensed construction activities, widespread informal and unauthorized housing developments were observed, especially on jointly owned lands. The buildings evaluated in this study were mostly constructed between 1970 and 1980.

In the scope of this study, a total of 536 buildings located in the Demetevler, Demetlale, Demetgül, and Demet neighborhoods were assessed using the street-level rapid visual screening (RVS) method. The construction years of the buildings are given in Figure 13.

2.3.11. Visual Screening Limitations

Considering that the Demetevler district of Yenimahalle, where multi-storey buildings have proliferated since the 1950s, features substandard construction materials (such as concrete and reinforcing steel) and lacks adequate engineering services and supervision, a rapid risk assessment was conducted on selected buildings to determine their vulnerability in the event of a potential earthquake. Based on these evaluations, a detailed structural

analysis was performed as a case study on one of the identified high-risk buildings to determine its damage states.

Despite their practicality for large-scale inventories, rapid screening methods inherently entail certain limitations. Primarily, evaluations rely on exterior visual observations (such as storey height, overhangs, structural type, and overall damage state), meaning that internal framing details, reinforcement quality, and material degradation cannot be directly assessed.

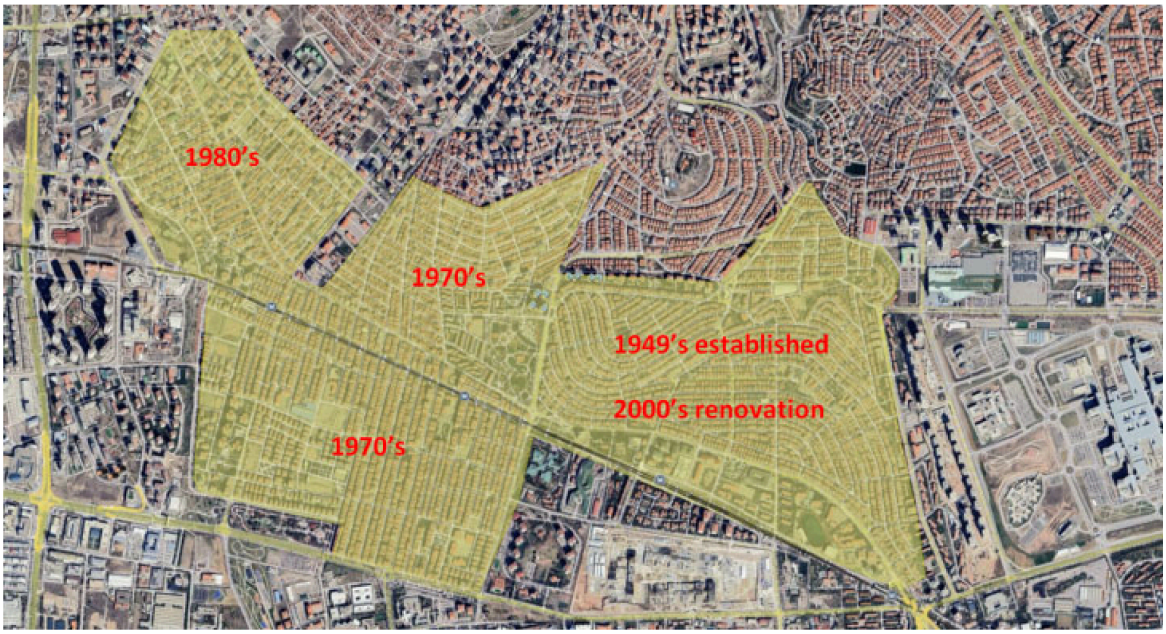


Figure 13. The years of construction of the region.

3. Findings of Field Study

A total of 536 buildings in the Demetevler region have been assessed. Field surveys were conducted for each building, and relevant data were recorded on pre-prepared assessment forms. Subsequently, corresponding scores were assigned based on predefined evaluation tables, and a total score was calculated for each building. The analysis of the collected data is presented in this section. Based on the assessment results, a threshold score of 50 points was established for the evaluated buildings. Structures scoring below this threshold are considered to be at high risk. The scores of the buildings are shown in Figure 14. The 50-point risk score threshold originates from the original calibration of the Sucuoğlu and Yazgan method.

Out of the 536 buildings assessed in the Demetevler region, 252 were identified as high-risk, while 284 were classified as low-risk for a risk score of 50. Figures 14 and 15, and Figure 16 illustrate the percentage distribution of buildings with risk scores below and above 45, 50, and 55, respectively.

3.1. Distribution of Buildings by Number of Storeys and Their Performance Ratios

It is observed that high-rise buildings are predominant in the region. Figure 17 shows the distribution of buildings according to the number of floors. The examined buildings have been constructed in very close proximity to one another. Accordingly, it is anticipated that post-disaster evacuation planning in the area would be challenging.

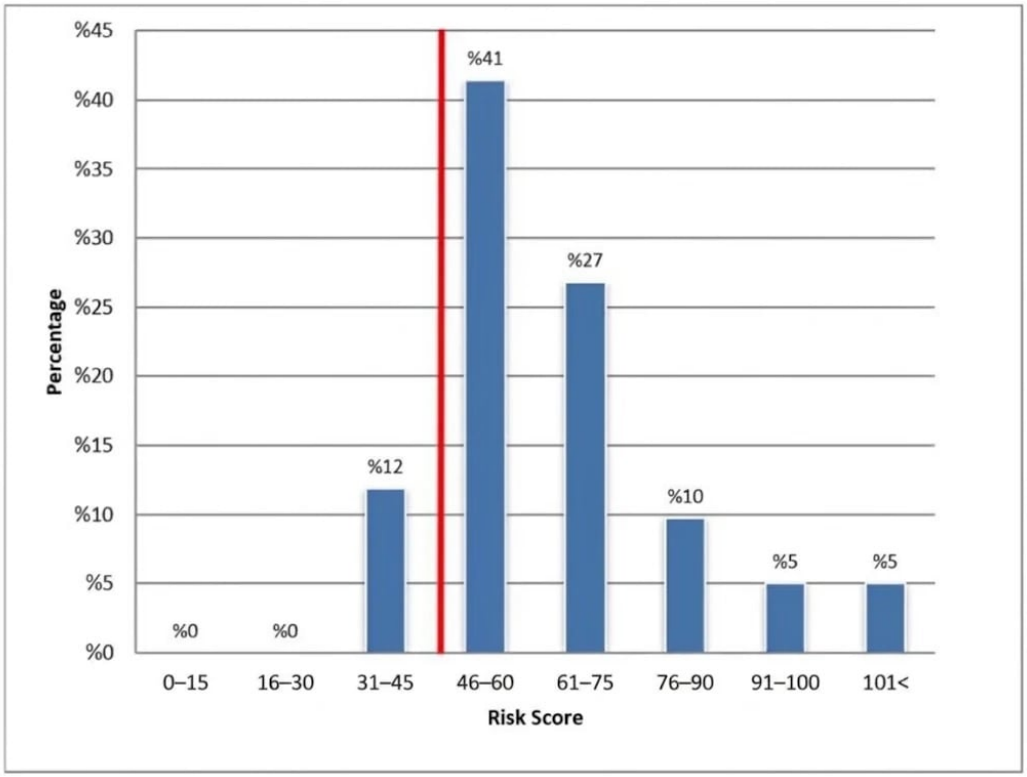


Figure 14. Distribution of buildings according to the threshold score of 45.

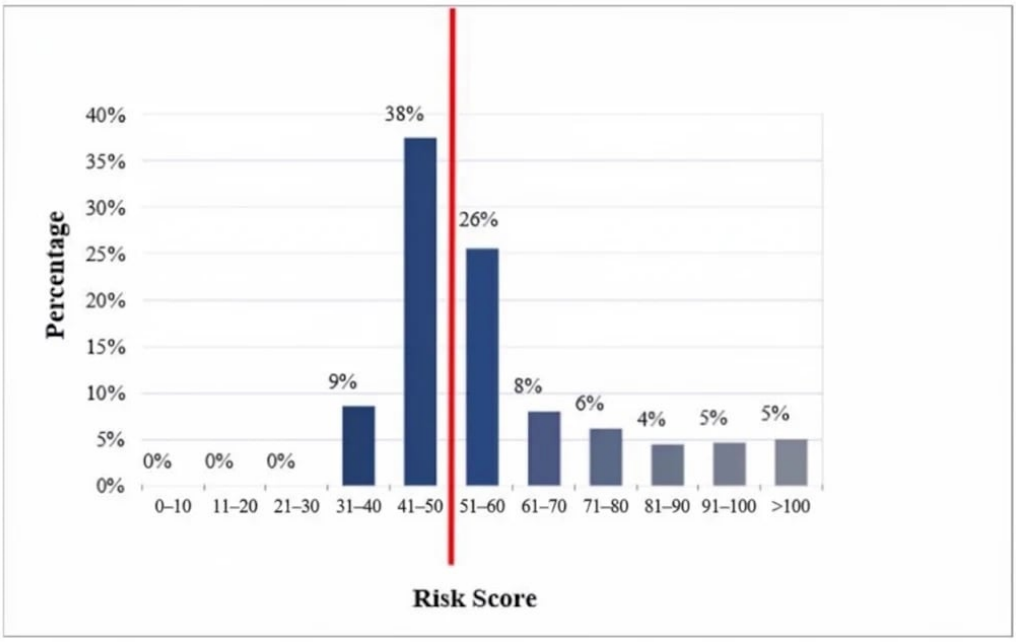


Figure 15. Distribution of buildings according to the threshold score of 50.

As illustrated in Figure 18, the risk level in buildings with six or more storeys was determined to exceed 50%. It has been observed that the risk levels tend to increase with the number of storeys in the assessed buildings. Depending on the number of storeys of the buildings, their risk status is presented in Figure 18.

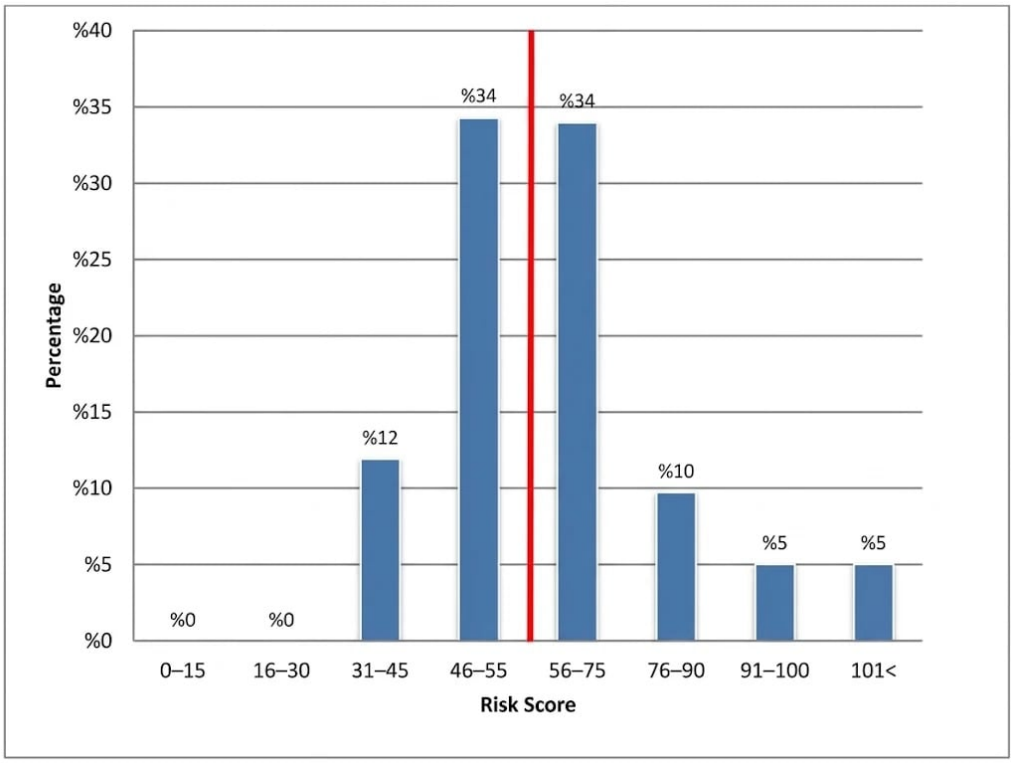


Figure 16. Distribution of buildings according to the threshold score of 55.

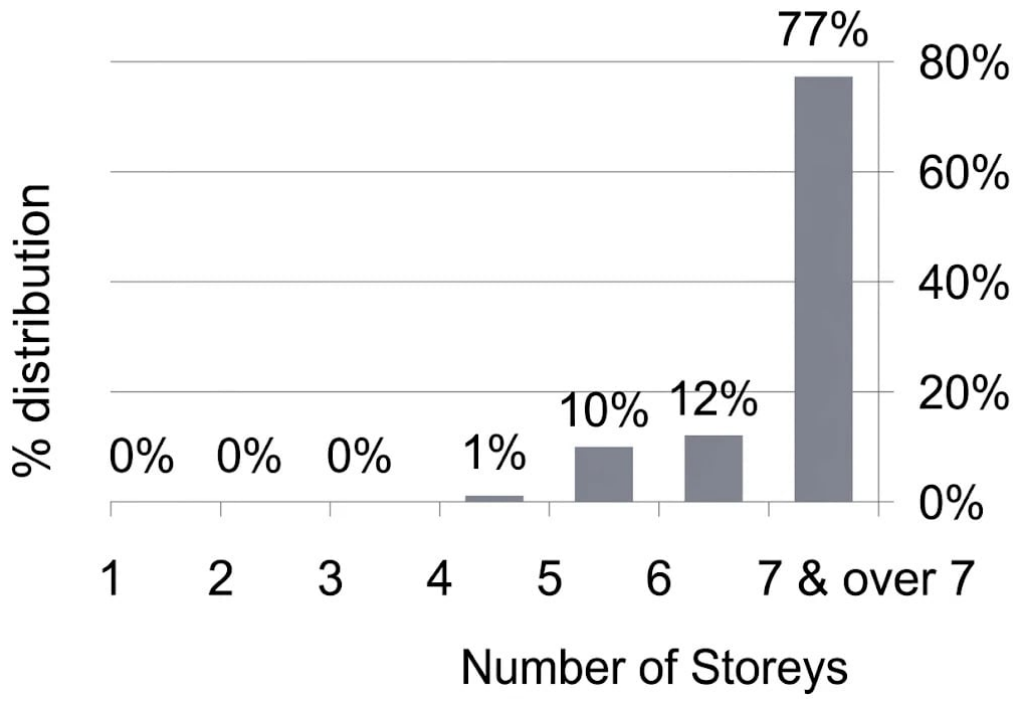


Figure 17. Distribution of buildings by number of floors.

The correlation between building height and structural vulnerability underscores the remarkably high risk profile of the region. While buildings with five or fewer storeys generally present low risk levels, the high-risk ratio escalates significantly to 55% for structures with six or more storeys. Crucially, the vast majority of the surveyed building stock (89%) falls precisely into this vulnerable category.

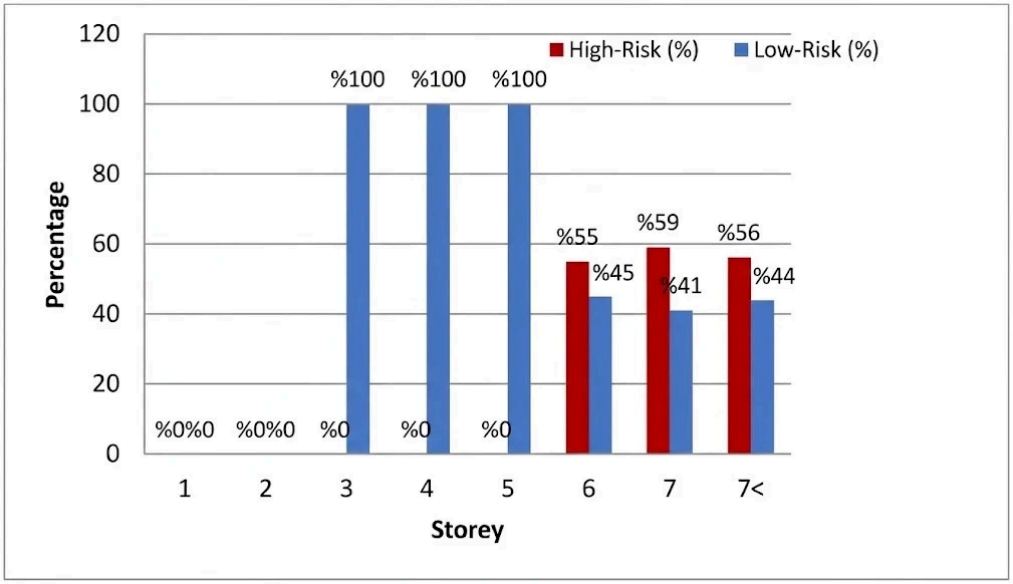


Figure 18. Distribution of high-risk buildings according to number of storeys.

3.2. Risk Distributions of Buildings with Heavy Overhangs

In buildings with heavy overhangs, it is seen in Figure 19 that the total risk score decreases more as the number of storeys increases. An increase in the number of storeys leads to a higher total structural weight, which in turn results in greater shear forces acting on the building.

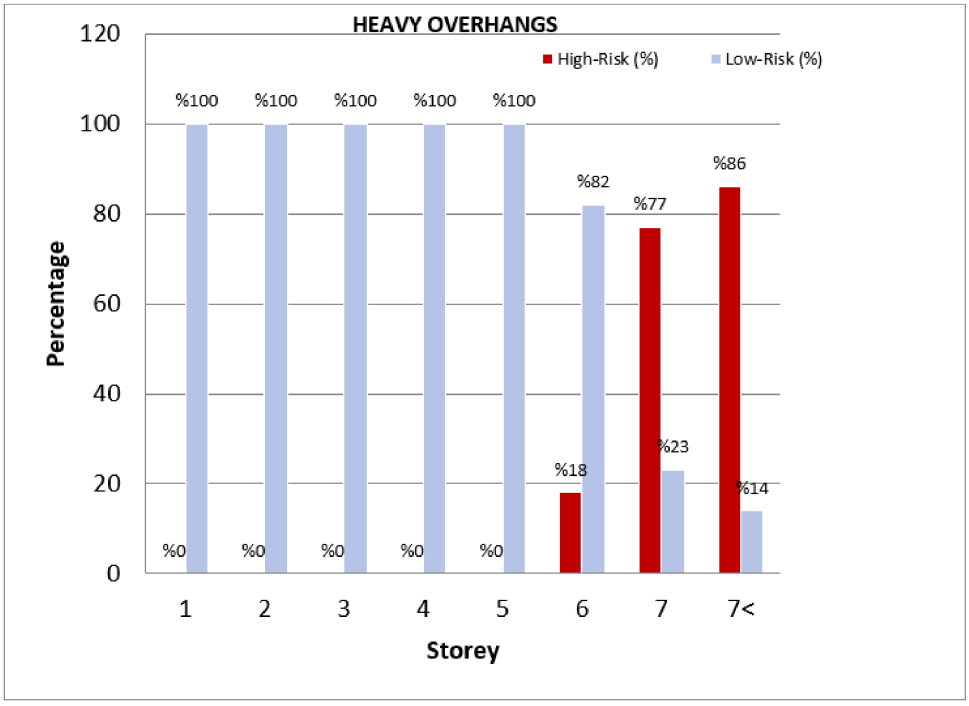


Figure 19. Risk distributions of buildings with heavy overhangs.

3.3. Risk Distribution of Soft-Storey Buildings

Structures with soft storeys exhibit a similar distribution pattern to those with heavy overhangs, and the associated risk tends to increase with building height. Risk distributions of buildings with soft storeys are illustrated in Figure 20.

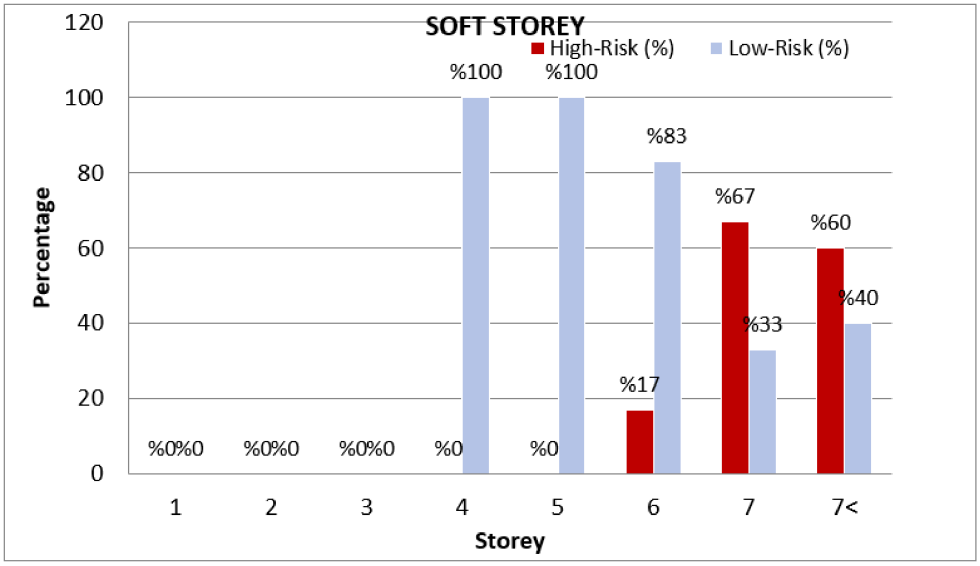


Figure 20. Risk distributions of buildings with soft storeys.

3.4. Risk Distribution of Buildings with Short Columns

The presence of short columns in buildings has been recognized as a structural deficiency that elevates earthquake risk. The risk distribution of short-column buildings based on the number of storeys is presented in Figure 21. Due to the concentration of high shear forces, short columns are particularly susceptible to brittle failure.

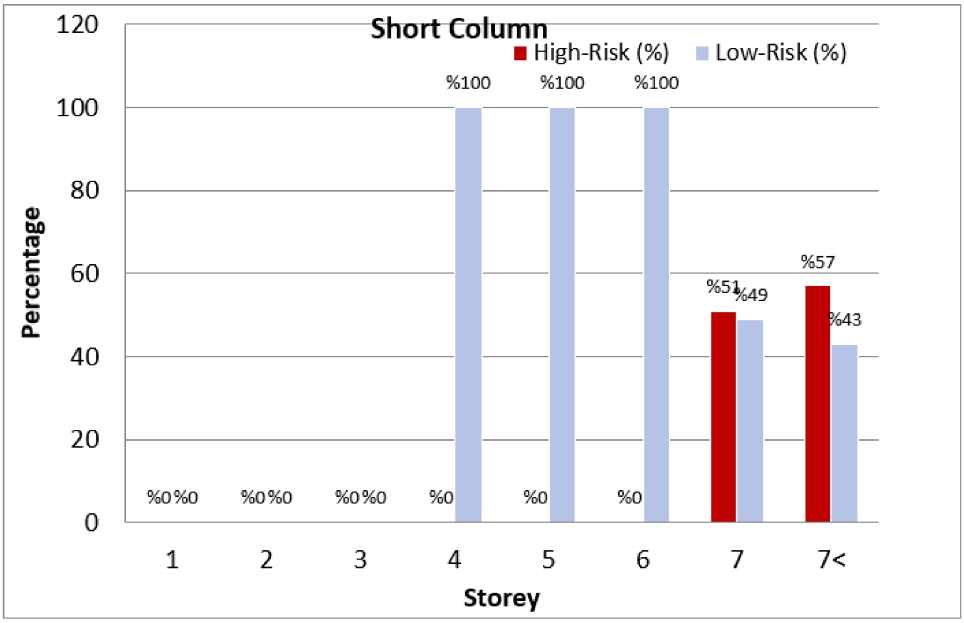


Figure 21. Risk distribution in buildings with short columns.

3.5. Building Risk Distribution of Pounding Effect

The pounding effect risk distribution according to storey number is illustrated in Figure 22. It has been determined that the pounding effect influences the risk status by more than 50% for buildings with six or more storeys.

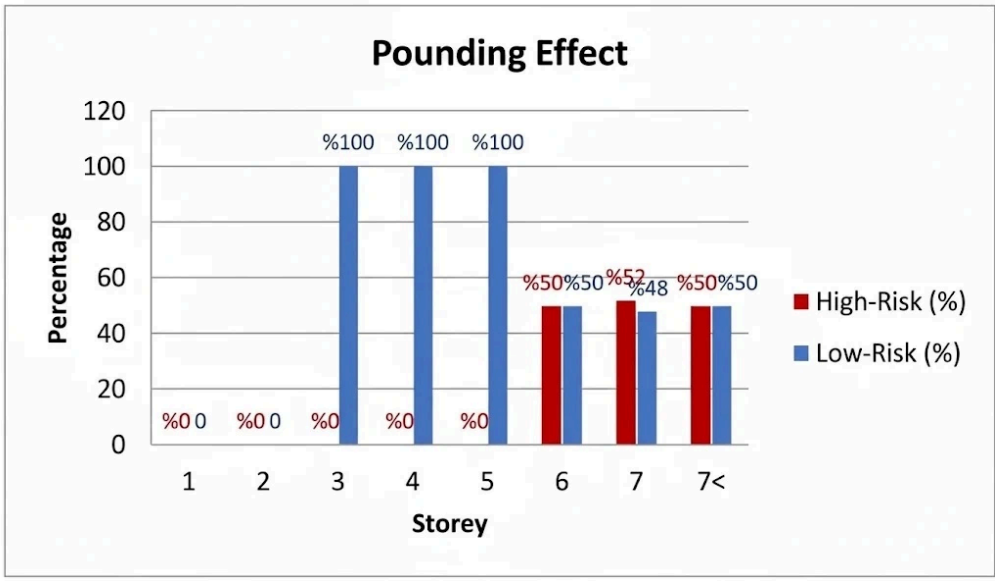


Figure 22. Risk distribution of pounding effect on buildings.

3.6. Risk Ratios of Buildings Located on Sloping Terrain

The rate of risky structures on sloping land was determined to be approximately 54%. The risk status is given in Figure 23.

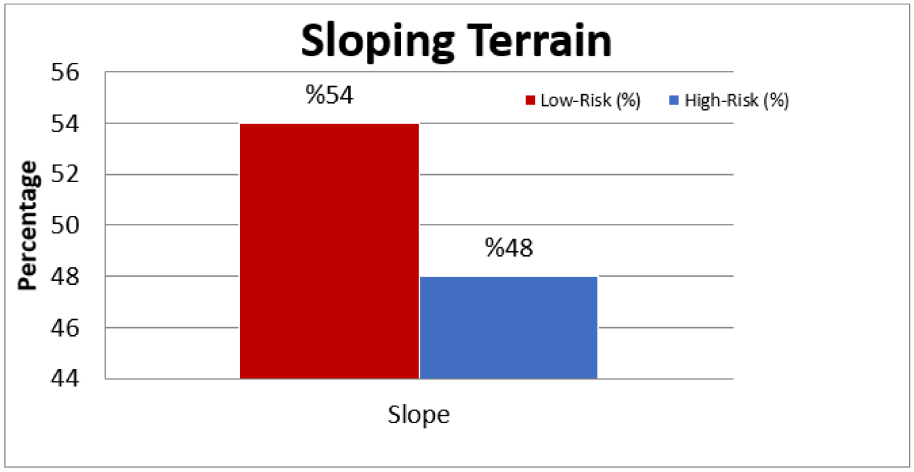


Figure 23. Risk distribution of buildings located on sloping terrain.

3.7. Impact of Visual Quality on Building Risk Assessment

This parameter reflects the perceived construction quality based on the observable exterior features of the building and directly influences the risk score. The construction date and the historical period in which the building was constructed are considered significant indicators of structural quality. In this context, conducting interviews with individuals who witnessed the construction process is deemed beneficial for a more accurate evaluation of this parameter. Building quality risk distributions for four, five, six, seven, and over seven storeys are illustrated in Figures 24–28, respectively.

Observations indicate that some buildings regarded as having good construction quality still exhibit risk scores exceeding critical thresholds. In contrast, for structures identified as poorly constructed, seismic risk tends to increase proportionally with the number of storeys. Figures 24–28 demonstrate that construction quality exerts a decisive influence on structural seismic performance.



Figure 24. Building quality risk distribution in 4-storey buildings.



Figure 25. Building quality risk distribution in 5-storey buildings.



Figure 26. Building quality risk distribution in 6-storey buildings.



Figure 27. Building quality risk distribution in 7-storey buildings.



Figure 28. Building quality risk distribution in 7-storey and above buildings.

3.8. Building Risk Score Analysis Report

3.8.1. General Statistics

A total of 536 buildings were evaluated in the dataset. Considering the entire building stock, the following was observed:

- Mean Risk Score (μ): 59.48.
- Standard Deviation (σ): 20.07.

3.8.2. Distribution Plot

Figure 29 below illustrates the frequency distribution (histogram) of the building risk scores fitted with a normal distribution curve. The 50-point risk threshold is highlighted with a red dashed line.

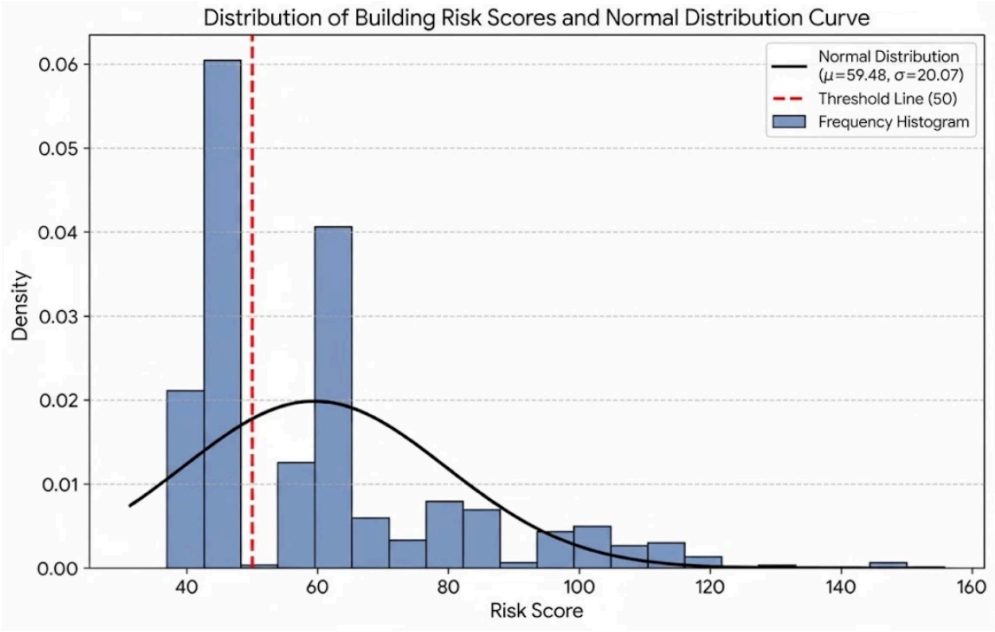


Figure 29. Distribution of building risk scores and normal distribution curve.

3.8.3. Risk Group Statistics (Threshold: 50 Points)

Buildings were categorized into two distinct risk groups based on the 50-point threshold. The high-risk group (score ≤ 50) comprises a total of 247 buildings, with a mean score of 43.78 and a standard deviation of 2.19. Conversely, the low-risk group (score > 50) includes 289 buildings, exhibiting a mean score of 72.90 and a standard deviation of 18.76.

3.9. Evaluation Based on Building Location

A total of 536 buildings were surveyed through field screening. The evaluation covered 232 buildings in Demetevler, 117 in Demetgül, and 187 in Demetlale. As a result of this study, 252 buildings were identified as falling into the high-risk category, with total risk scores below 50 points. A clear correlation was observed between an increase in the number of storeys and a higher structural risk level. This study also investigated the influence of building locations on seismic risk. The assessed buildings were mapped and color-coded based on their risk score ranges to visually represent spatial risk distribution. Figure 30 illustrates risk score ranges of investigated buildings on the map.

Buildings marked in red indicate high-risk structures with a total risk score below 50 points in Figure 28. The construction quality and architectural characteristics of these buildings often reflect the typical features of the urban development phases during which the respective residential areas were zoned. The design decisions made, the level of enforcement during the construction phase, and the construction technologies available at the time have collectively contributed to the common characteristics observed in these buildings. In this context, the Demetevler region exhibits several well-known structural and architectural patterns, including the following characteristic and static features:

These common characteristics observed in the Demetevler region include the following:

- Permitting of high-rise building construction, often without strict height limitations.
- Use of manually mixed concrete during the construction phase, rather than ready-mix concrete.
- Absence of any foundation waterproofing or insulation systems in the structural base.
- Lack of formal construction supervision and inspection during the building process.
- Design of many ground floors as commercial units, increasing occupancy loads and functional irregularity.

- Construction of tall buildings in very close proximity to one another, leading to insufficient separation distances and increased seismic interaction risk.

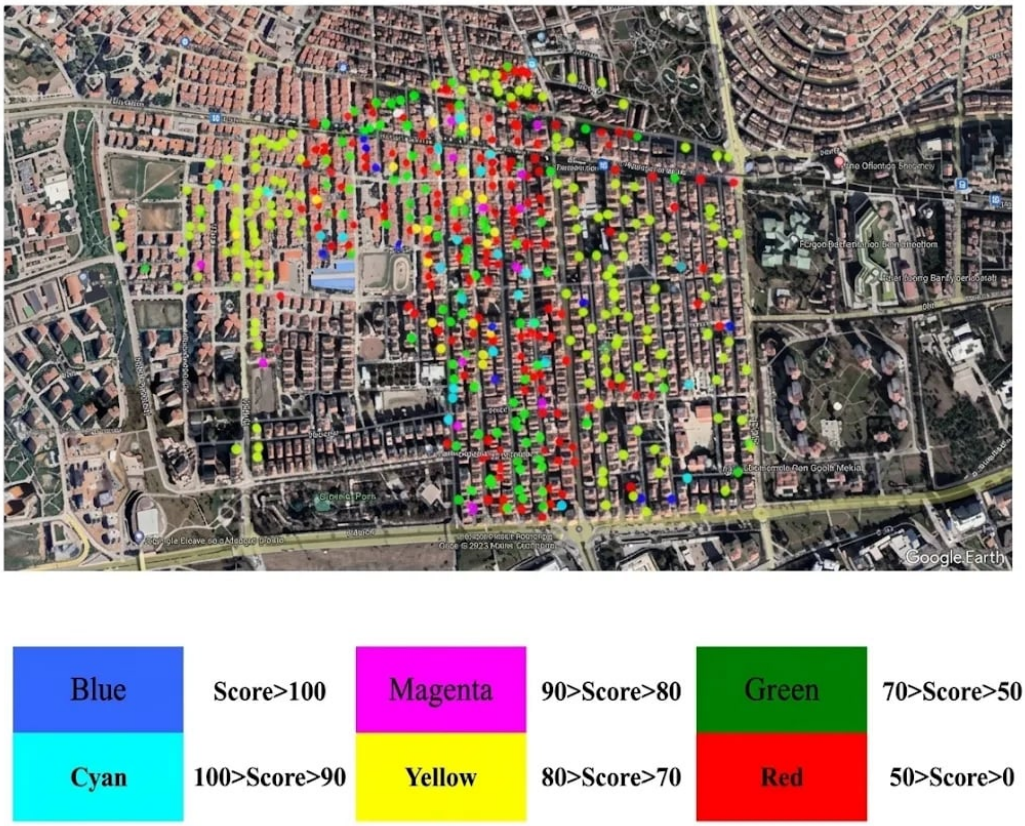


Figure 30. Aerial photograph annotated according to risk scores.

3.10. Sensitivity Analysis Based on Risk Score

A sensitivity analysis was conducted to investigate the effect of the selected cut-off threshold on the risk classification of the building stock within the distribution of building risk scores in rapid visual screening methods (e.g., the **Sucuoğlu & Yazgan** method).The risk status of the buildings for risk scores of 45, 50, and 55 is given in Table 3.

The sensitivity index calculation (S_R) is is presented in Equation (2).

$$S_R = \frac{\Delta\%\text{High} - \text{Risk Buildings}}{\Delta R_{\text{threshold}}} \quad (2)$$

The sensitivity ratio was computed by measuring the relative change in the percentage of prioritized high-risk structures ($\Delta\%\text{High} - \text{Risk}$) divided by the shift in the cut-off score ($\Delta R_{\text{threshold}}$). This metric assesses the robustness of the rapid screening classification against threshold variability.

To evaluate the robustness of the rapid visual screening methodology and its sensitivity to threshold selection, a sensitivity analysis was conducted for cut-off risk scores of 45, 50, and 55. When a cut-off threshold of 55 is adopted, 54% of the evaluated building stock is classified as high-risk, while 46% remains in the low-to-moderate risk category. Lowering the threshold to 45 shifts borderline structures into the high-risk category, noticeably increasing the prioritized building ratio. This distribution highlights that a substantial portion of the building stock is concentrated near the critical threshold (e.g., 34–41% in the 46–60 risk range), demonstrating high sensitivity to threshold shifts and confirming that a cut-off score around 50–55 provides a balanced benchmark for urban prioritization strategies.

Table 3. Risk scores and assessment.

Risk Cut-Off Threshold (Rthreshold)	High-Risk Building Ratio (%)	Low-to-Moderate-Risk Ratio (%)	Characteristic Assessment & Structural Interpretation
Rthreshold = 45	54%	46%	Conservative Approach: Classifies more than half of the building stock as high-risk by incorporating borderline structures (31 ≤ risk score ≤ 45).
Rthreshold = 50	88%	12%	High-Sensitivity Benchmark: Captures all structures with scores above 45, highlighting the concentration of buildings in the critical 46–60 risk interval.
Rthreshold = 55	54%	46%	Balanced Prioritization Cut-Off: Provides a distinct mid-spectrum boundary that evenly segregates the building stock into high and moderate/low priority tiers.

4. Modeling of a Structure Located in the Region

After the field studies and evaluation of the obtained data, it was aimed to evaluate the data obtained from the street with the rapid scanning method with real building examples. The static and architectural projects of the buildings located on the immovable property with a surface area of 316 m^2 in Demetlale neighborhood were obtained from Yenimahalle Municipality. In line with the obtained projects, the buildings were modeled in the Sap2000 program, and a single-mode pushover analysis was performed.

When the projects related to the structure are examined, it is clearly seen that there are irregularities/defects in the structure, such as weak floors, heavy cantilevers, short columns, and topographic effects, which are determined as negative parameters in the rapid street-assessment method from the street. The total score of the structure was determined as 40 as a result of this method. Photographs of the relevant structure are shown in Figure 31. 3D modeling views are shown in Figure 32.



Figure 31. Front and right view photographs of the building.

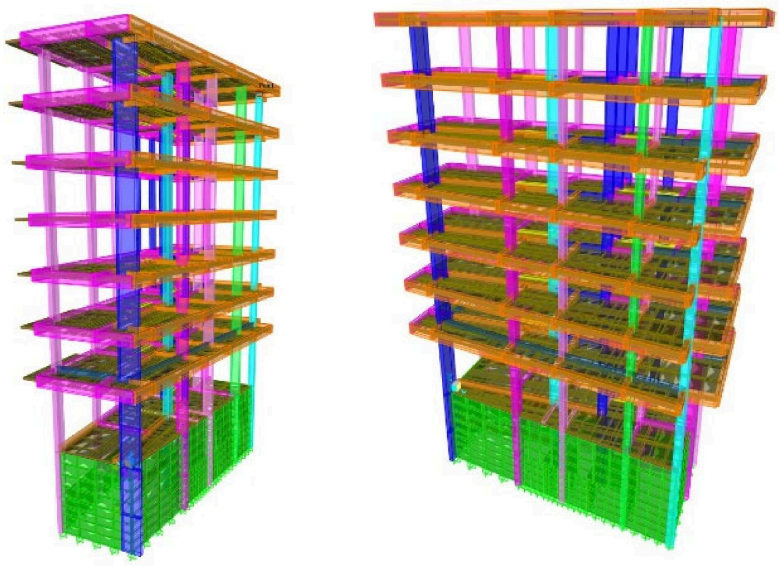


Figure 32. 3D modeling of the building.

In the 3D model view, light blue, dark blue, and pink vertical elements represent columns; dark pink and light brown horizontal elements represent beams; dark green vertical elements represent basement walls.

Section drawing and architectural plan of 1–6 floors and formwork plan modeling of 1–6 normal floors are illustrated in Figures 33 and 34, respectively.

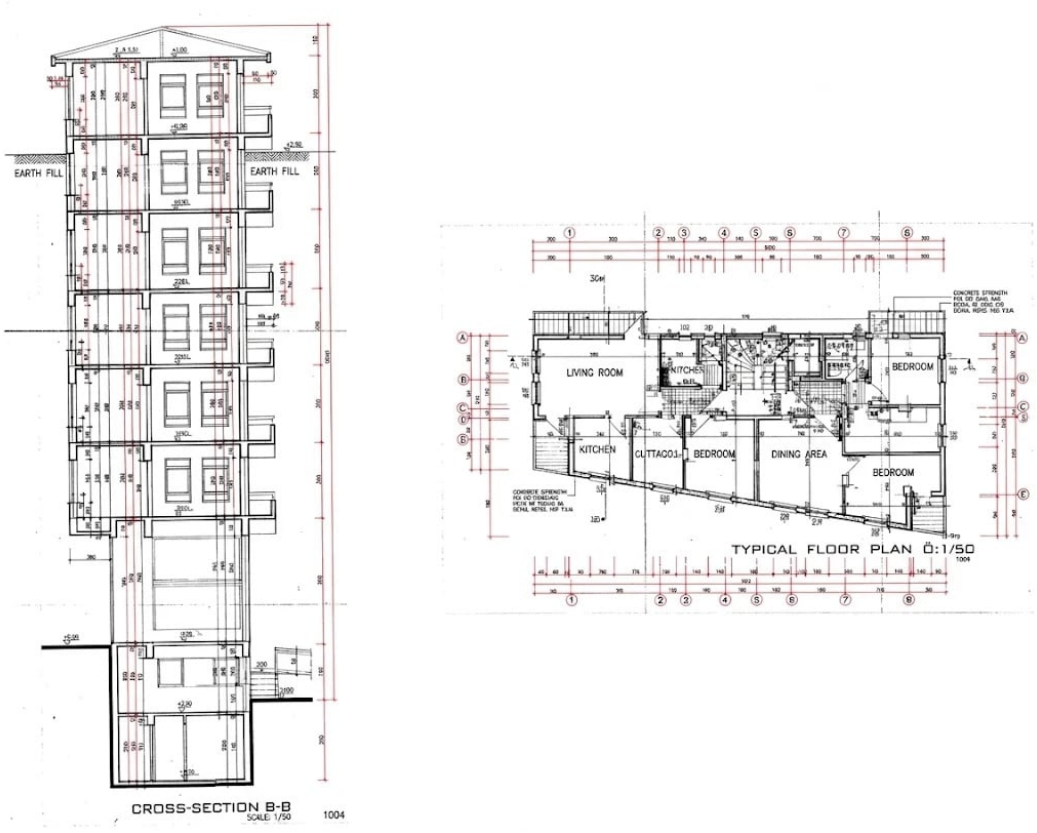


Figure 33. Section drawing and architectural plan of 1–6 floors.

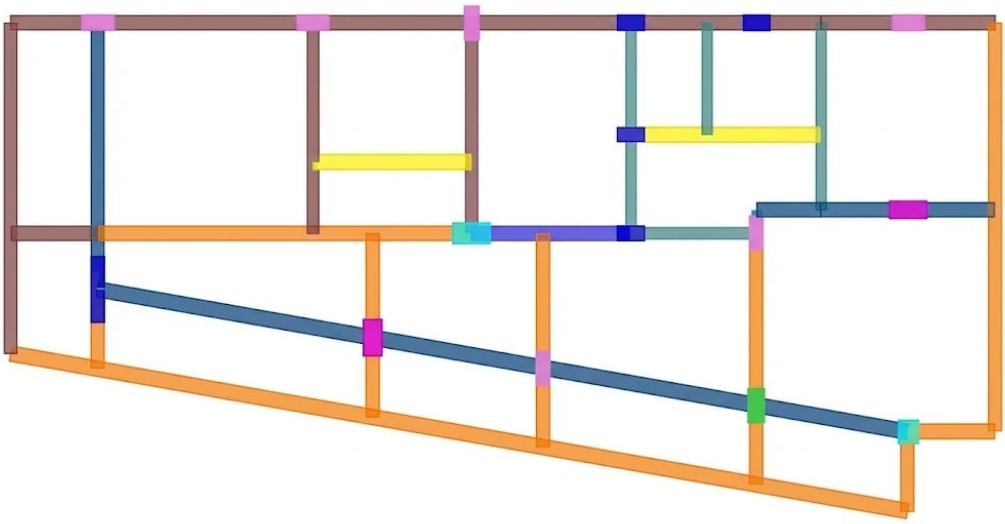


Figure 34. Formwork plan modeling of 1–6 normal floors.

In the plan view, light pink, dark pink, light blue, dark blue, and green elements represent columns, whereas dark brown, light brown, yellow, and dark green elements denote beams.

Utilizing Table 2 and Equation (1), the risk score of the modeled structure was evaluated and listed in Table 4.

Table 4. Risk score of modeled structure.

	Score
Initial Score	95
Soft Storey (SS)	−20
Heavy Overhangs	−15
Visual Quality	−15
Pounding Effect	0
Topographic Effect	0
Total Score	40

4.1. Data Related to Analysis

The obtained projects were used in determining the analysis parameters of the modeled structures. The soil class was ZD from previous investigations in the region. The structural design characteristics are shown in Table 5. The C16 concrete and S220 steel classes used in the analyses represent the minimum concrete and reinforcement strengths based on the current specifications and regulations in force in Turkiye [35,36]. Furthermore, considering the local ground conditions, the soil class corresponds to the medium-dense/medium-stiff category.

The column dimensions and reinforcement details are given in Table 6, while the beam dimensions and reinforcement details are presented in Table 7.

To evaluate the strength and deformation characteristics of the structure under seismic actions, a nonlinear static pushover analysis was performed. This method requires a fully detailed structural design prior to analysis. Gravity loads were defined using the G + 0.3Q combination in accordance with the Turkish Building Earthquake Code [36] to calculate the lateral seismic forces. Floor diaphragms were modeled as rigid at each level. The resulting pushover curves in the X and Y directions were presented in terms of base shear force versus roof displacement. Using the modal capacity diagram derived from the pushover analysis,

the modal displacement demand was calculated based on the spectral displacement demand determined according to the seismic code. The plastic rotation demands at the plastic hinges were then compared against the performance level damage limits to identify *the section* performance states. In the nonlinear static analysis, lumped plastic hinges were assigned to all structural beam and column elements. The building was incrementally pushed to an initial roof displacement corresponding to a maximum of 4% of the total structural height to establish the capacity curve. The target displacement demand was determined at the intersection of the capacity diagram and the demand spectrum, after which the structure was pushed to this target displacement to complete the demand assessment. Element damage states were categorized into three performance levels based on the plastic rotation demands at element ends: limited damage (LD), defined by initial steel yielding or micro-cracking with minimal damage requiring no structural repair; controlled damage (CD), characterized by post-yield inelastic deformations and concrete crushing without rebar buckling, representing repairable damage that may necessitate structural intervention; and collapse prevention (CP), corresponding to a significant reduction in load-carrying capacity at the ultimate rotation limit, beyond which the element fails to safely sustain shear or axial loads, posing a critical risk of partial or global collapse.

Table 5. Structural design characteristics.

Geometric Properties	Width	9.05 m
	Length	18.00 m
	Number of floors	2B + Z + 6
Material Properties	Concrete grade	C16
	Steel Grade	S220
Load definitions	Live load	200 kg/m^2
	Dead load	150 kg/m^2
	Wall Load	900 kg/m
	Live load reduction factor	0.3
Soil Properties	Soil class	ZD
	Spectral Acceleration Coefficient	0.339

Table 6. Column section dimensions and longitudinal reinforcements.

Section	b (mm)	h (mm)	Longitudinal Reinforcement	Total Longitudinal Reinforcement Area (mm^2)
1	250	600	8Ø16	1600
2	250	1180	16Ø16	3200
3	350	700	14Ø16	2800
4	300	600	10Ø16	2000

Table 7. Beam section dimensions and longitudinal reinforcement.

No	Dimensions		Bottom Rebar			Top Rebar		
	Width (bw) mm	Length (h) mm	No	Dia. (mm) Ø	Area (mm^2)	No	Dia. (mm) Ø	Area (mm^2)
1	200	400	4	12	450	2	12	230
2	200	500	5	12	570	3	12	340
3	200	600	6	12	680	3	12	340
4	230	500	6	12	680	3	12	340

Table 7. *Cont.*

No	Dimensions		Bottom Rebar			Top Rebar		
	Width (bw) mm	Length (h) mm	No	Dia. (mm) Ø	Area (mm^2)	No	Dia. (mm) Ø	Area (mm^2)
5	230	600	7	12	790	4	12	450
6	250	500	6	12	680	3	12	340
7	250	600	7	12	790	4	12	450
8	250	700	9	12	1020	4	12	450
9	300	300	4	12	450	2	12	230
10	350	500	9	12	1020	4	12	450

4.2. Findings of Modelling

The building modeled in this study was evaluated based on design values derived from the single-mode pushover analysis in accordance with the current seismic code [36]. The modeled building is approximately 35 years old. Pushover analysis results in the X and Y directions are summarized in Tables 8 and 9, respectively.

Pushover and modal capacity curves of the building in the X and Y directions are shown in Figures 35 and 36, respectively. The maximum base shear force is approximately 3050 kN; the top displacement is 0.10 m for the pushover curve, and the maximum base shear force is approximately 2500 kN; the top displacement is 0.08 m for the modal capacity curve.

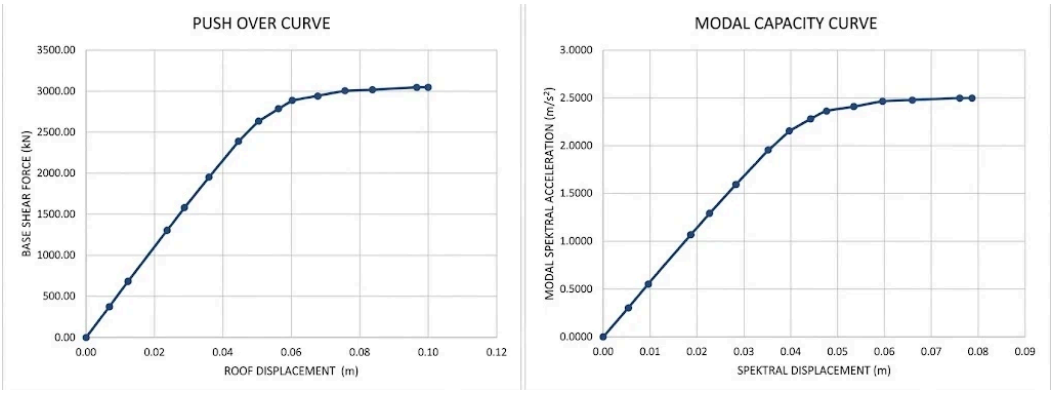


Figure 35. Pushover and modal capacity curves of the building in the X direction.

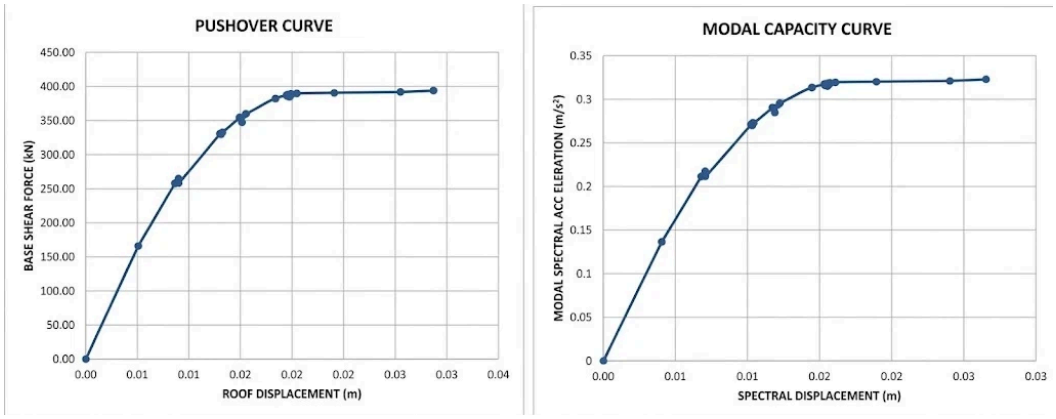


Figure 36. Pushover and modal capacity curves of the building in the Y direction.

Table 8. Pushover analysis results in the X direction for the building.

Pushover Curve			Capacity Curve	
Step	**Displ (m)**	**Force (kN)**	**SD (m)**	**SA (m/sn²)**
1	0.000	0.000	0	0.0000
2	0.007	373.000	0.0054	0.3059
3	0.012	681.672	0.0095	0.5590
4	0.024	1311.900	0.0186	1.0758
5	0.029	1582.000	0.0225	1.2973
6	0.036	1955.000	0.0283	1.6032
7	0.045	2392.300	0.0351	1.9618
8	0.050	2636.600	0.0397	2.1621
9	0.056	2791.000	0.0443	2.2887
10	0.060	2891.000	0.0476	2.3707
11	0.068	2945.400	0.0534	2.4153
12	0.076	3009.600	0.0596	2.4680
13	0.084	3022.500	0.0659	2.4785
14	0.097	3048.230	0.0761	2.4996
15	0.100	3048.230	0.0787	2.4996

Table 9. Pushover analysis results in the Y direction for the building.

Pushover Curve			Capacity Curve	
Step	**Displ (m)**	**Force (kN)**	**SD (m)**	**SA (m/sn²)**
1	0.000	0.000	0	0.0000
2	0.005	166.084	0.0040	0.1362
3	0.009	257.992	0.0068	0.2116
4	0.009	257.751	0.0068	0.2114
5	0.009	257.751	0.0068	0.2114
6	0.009	257.749	0.0068	0.2114
7	0.009	257.837	0.0068	0.2114
8	0.009	265.385	0.0071	0.2176
9	0.009	258.187	0.0071	0.2117
10	0.013	330.543	0.0102	0.2711
11	0.013	331.934	0.0103	0.2722
12	0.013	331.427	0.0103	0.2718
13	0.013	331.427	0.0103	0.2718
14	0.013	331.454	0.0103	0.2718
15	0.013	333.186	0.0104	0.2732

Peak displacement has been determined using the data presented in Table 10. Peak displacement is approximately 0.04 m.

Table 10. Determination of the performance point of the structure.

SDE Elastic displ (m)	0.034
SDİ İnelastic disp (m)	0.034
Modal parameter (ϕ)	0.0257
Modal participation factor (Γ)	49.37
Peak displacement (m)	0.0437

The performance point of the structure is shown in Figure 37.

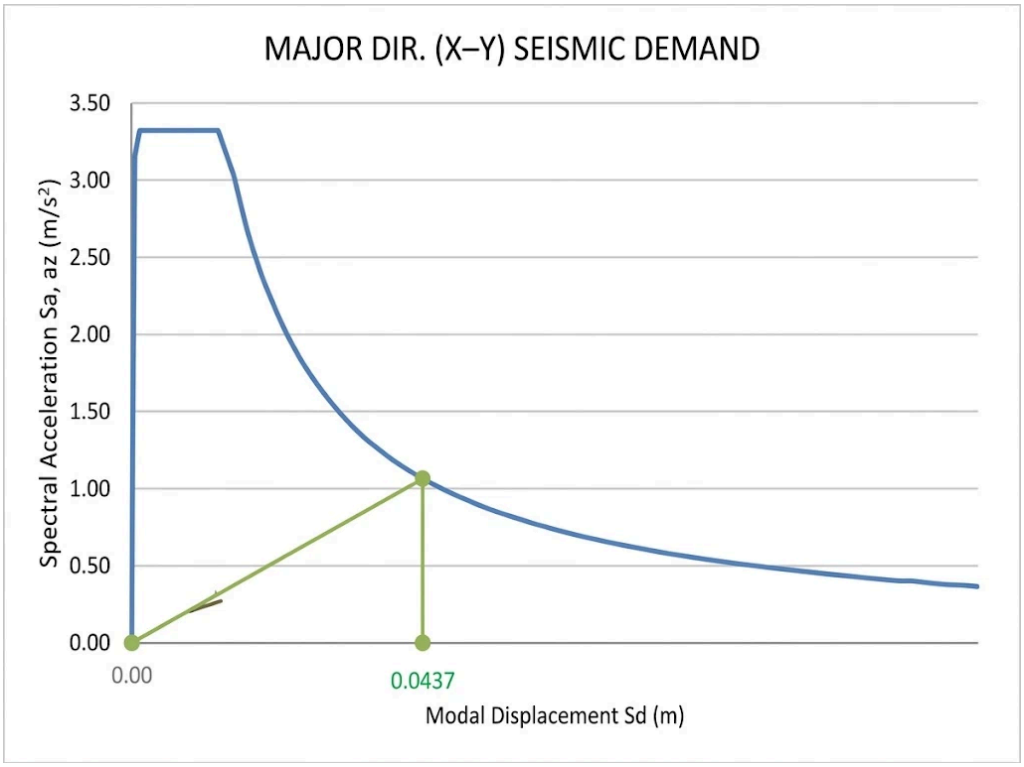


Figure 37. Performance point of the structure in the Y direction.

The damage state of the elements is given in Table 11.

Table 11. Damage states of structural elements.

El. No	Load	Rotation Φ_{RD}	Φ_{PF}	Φ_{CD}	Result
1148	P-Y	0.000235	0.000272	0.000204	CD
1150	P-Y	0.000289	0.000272	0.000204	CP
1208	P-Y	0.000042	0.000272	0.000204	LD
1208	P-Y	0.000256	0.000272	0.000204	CD
1209	P-Y	0.000756	0.000272	0.000204	CP
1222	P-Y	0.000387	0.000272	0.000204	CP
1250	P-Y	0.000131	0.000272	0.000204	LD
1251	P-Y	0.000131	0.000272	0.000204	LD
1263	P-Y	0.000276	0.000272	0.000204	CP
1304	P-Y	0.000117	0.000272	0.000204	LD
1679	P-Y	0.00004	0.000272	0.000204	LD
1680	P-Y	0.000222	0.000272	0.000204	CD
1681	P-Y	0.000426	0.000272	0.000204	CP
1682	P-Y	0.000514	0.000272	0.000204	CP
1704	P-Y	0.000616	0.000272	0.000204	CP
1704	P-Y	0.001023	0.000272	0.000204	CP
1716	P-Y	0.000035	0.000272	0.000204	LD
1717	P-Y	0.007575	0.000272	0.000204	CP
1717	P-Y	0.006728	0.000272	0.000204	CP
1726	P-Y	0.00012	0.000272	0.000204	LD
1726	P-Y	0.000153	0.000272	0.000204	LD
1735	P-Y	0.000116	0.000272	0.000204	LD
1735	P-Y	0.000112	0.000272	0.000204	LD
1744	P-Y	0.006467	0.000272	0.000204	CP
1744	P-Y	0.005642	0.000272	0.000204	CP

Table 11. *Cont.*

El. No	Load	Rotation Φ_{RD}	Φ_{PF}	Φ_{CD}	Result
1753	P-Y	0.00005	0.000272	0.000204	LD
1753	P-Y	0.000023	0.000272	0.000204	LD
1762	P-Y	0.000058	0.000272	0.000204	LD
1762	P-Y	0.000017	0.000272	0.000204	LD
1771	P-Y	0.000053	0.000272	0.000204	LD
1771	P-Y	0.000097	0.000272	0.000204	LD
1780	P-Y	0.00009	0.000272	0.000204	LD
1780	P-Y	0.000141	0.000272	0.000204	LD
1781	P-Y	0.000005262	0.000272	0.000204	LD
1781	P-Y	0.00000423	0.000272	0.000204	LD
1789	P-Y	0.000002643	0.000272	0.000204	LD
1789	P-Y	0.000017	0.000272	0.000204	LD
1798	P-Y	0.000013	0.000272	0.000204	LD
1798	P-Y	0.000017	0.000272	0.000204	LD
1807	P-Y	0.006839	0.000272	0.000204	CP
1807	P-Y	0.00584	0.000272	0.000204	CP
1816	P-Y	0.000144	0.000272	0.000204	LD
1816	P-Y	0.000049	0.000272	0.000204	LD
1825	P-Y	0.000022	0.000272	0.000204	LD
1825	P-Y	0.000028	0.000272	0.000204	LD
1826	P-Y	0.000001312	0.000272	0.000204	LD
1826	P-Y	0.000002058	0.000272	0.000204	LD
1827	P-Y	4.356×10^{-8}	0.000272	0.000204	LD
1853	P-Y	0.000404	0.000272	0.000204	CP
1855	P-Y	0.00035	0.000272	0.000204	CP
1856	P-Y	0.001066	0.000272	0.000204	CP
1881	P-Y	0.000248	0.000272	0.000204	CD
1882	P-Y	0.0004	0.000272	0.000204	CP
1885	P-Y	0.000397	0.000272	0.000204	CP
1885	P-Y	0.00042	0.000272	0.000204	CP
1909	P-Y	0.000139	0.000272	0.000204	LD
1910	P-Y	0.000261	0.000272	0.000204	CD
1913	P-Y	0.000187	0.000272	0.000204	LD
1913	P-Y	0.000175	0.000272	0.000204	LD
1937	P-Y	0.000011	0.000272	0.000204	LD
1938	P-Y	0.000078	0.000272	0.000204	LD
1941	P-Y	0.000009585	0.000272	0.000204	LD
2071	P-Y	0.007211	0.000272	0.000204	CP
2071	P-Y	0.006516	0.000272	0.000204	CP
2072	P-Y	0.000187	0.000272	0.000204	LD
2080	P-Y	0.007162	0.000272	0.000204	CP
2080	P-Y	0.006632	0.000272	0.000204	CP
2081	P-Y	0.000031	0.000272	0.000204	LD
2081	P-Y	0.000138	0.000272	0.000204	LD
2089	P-Y	0.007045	0.000272	0.000204	CP
2089	P-Y	0.006544	0.000272	0.000204	CP
2090	P-Y	0.000097	0.000272	0.000204	LD
2096	P-Y	0.00068	0.000272	0.000204	CP

P-Y: pushover load in the Y direction. Φ_{RD}: plastic hinge rotation. Φ_{PF}: failure prevention limit rotation. Φ_{CD}: controlled damage limit rotation. CP: collapse prevention. LD: limited damage. CD: controlled damage.

In Table 11, if the rotation at the plastic hinge is between the controlled damage and failure prevention rotation limits ($\Phi_{CD} < \Phi_{RD} < \Phi_{PF}$), it is classified as controlled damage

(CD). If the plastic hinge rotation exceeds the failure prevention limit ($\Phi_{RD} > \Phi_{PF}$), it is denoted as collapse prevention (CP); if it is below the controlled damage limit ($\Phi_{RD} < \Phi_{CD}$), it is identified as limited damage (LD).

Structural element damages are given in Table 12. In total, 445 elements occurred, and 16% of them were damaged.

Table 12. Summary of structural element damage.

Summary of the Damage	
Number of controlled damaged elements	5
Number of limited damaged elements	41
Number of pre-collapse damaged elements	27
Total number of elements	445
Ratio of damaged element	16%

Model views of hinges are shown in Figure 38.

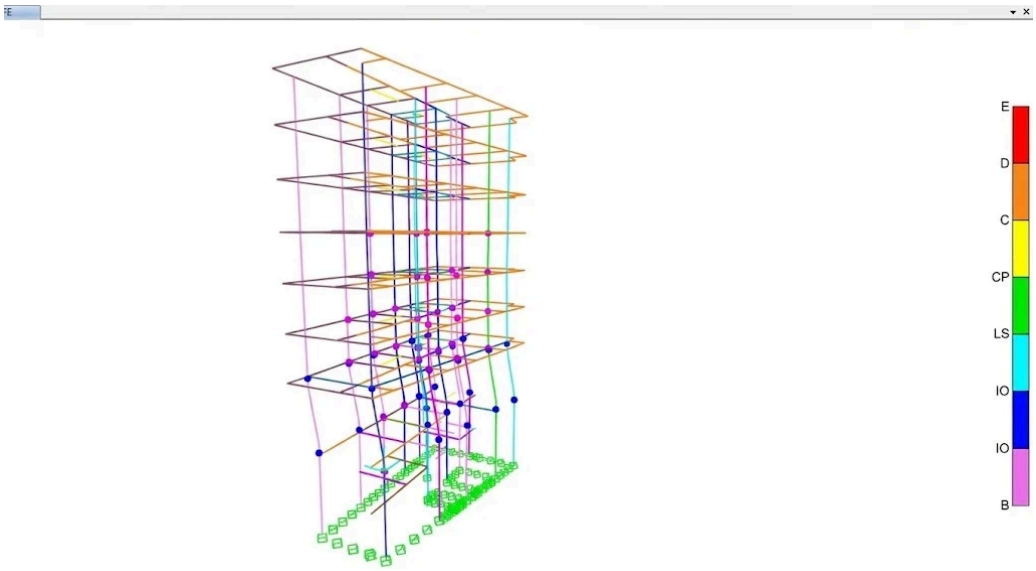


Figure 38. Model views of hinges.

5. Conclusions

In this study, 536 buildings located in the Demetevler neighborhood of Yenimahalle District, Ankara, were surveyed using the street-level rapid screening method. The collected data were evaluated in an office environment. It was determined that 47% of the surveyed buildings were classified as high-risk structures. The number of storeys and the ground acceleration value were observed to be the most influential factors affecting the risk level of the buildings. Buildings with up to six storeys were assessed as safe, while for buildings exceeding six storeys, the proportion of high-risk structures increased to 55%. It was also found that the number of storeys plays a significant role in the risk assessment of buildings with other structural defects:

- The proportion of buildings with six or more storeys in the surveyed area is as high as 89%. It can be concluded that the number of storeys is the most significant factor increasing the risk level of the buildings.
- Out of the 536 buildings, 47% (252 buildings) received a risk score below 50 (RS = 50), classifying them as high-risk structures. These buildings require detailed analysis, verification, and strengthening measures.

- The results indicate that structural deficiencies such as soft storeys, short columns, heavy overhangs, and poor construction quality increase the seismic risk of the buildings. It is crucial to establish regulations and control mechanisms that prevent the implementation of these structural deficiencies in newly zoned areas.
- It can be inferred that the urban development regime in the study area was established without full consideration of structural static and dynamic performance. Therefore, it would be beneficial to seek assistance and support from university expert teams before making new decisions.
- A field study was performed, and pushover analysis was applied to the real structure found to be at risk according to the risk scores, confirming its vulnerability through analytical results. In this respect, this study offers a feasible evaluation by combining the preliminary assessment and analysis phases on actual structures.
- The modeled structure is a building identified as risky through the rapid street survey. The purpose here is to demonstrate that a structure found to be risky via preliminary inspection also reaches a collapse state based on nonlinear behavior analysis results. Therefore, the rapid street survey method serves as a guide regarding the general condition of the structure.

The Yenimahalle district of Ankara is an area characterized by a high density of old buildings. This study is a field-based investigation in which visual evaluation, representing the initial stage of seismic risk assessment, was performed. It is crucial to conduct detailed inspections on structures identified as risky following the preliminary evaluation and to take necessary measures. These measures will ensure that potential earthquakes are weathered without damage or with minimal damage.

Additionally, because street-level surveys are conducted by different inspectors, observer subjectivity may introduce minor variances into the final risk scores. Furthermore, the framework relies on macro-level soil classifications, which may fail to capture site-specific microzonation details or soil–structure interaction effects for individual parcels. Finally, since rapid screening tools are predominantly calibrated for regular building typologies, the resulting scores can remain conservative or less reliable for structures featuring significant plan or vertical irregularities.

The method employed was evaluated by considering a risky building within the study area. The analysis revealed that the structure reaches a mechanism state, thereby demonstrating the validity of the method developed by Sucuoğlu and Yazgan [4,7,8].

The street survey conducted serves as a preliminary evaluation, providing insight into the general condition of the buildings. At this stage, buildings identified as potentially at risk will guide the prioritization of structures for detailed evaluation. This is a limitation of this study.

It is recommended that future studies focus on expanding this rapid screening methodology to a broader and more diverse building stock, encompassing various structural typologies and seismic zones.

Author Contributions: Conceptualization, Ş.B.E.; methodology, Ş.B.E.; validation, Ş.B.E. and R.S.E.; formal analysis, Ş.B.E. and R.S.E.; investigation, Ş.B.E. and R.S.E.; resources, Ş.B.E. and R.S.E.; data curation, Ş.B.E. and R.S.E.; writing—original draft preparation, Ş.B.E.; writing—review and editing, Ş.B.E.; visualization, Ş.B.E. and R.S.E.; supervision, Ş.B.E.; project administration, Ş.B.E. All authors have read and agreed to the published version of the manuscript.

Funding: This research received no external funding.

Data Availability Statement: The original contributions presented in this study are included in the article.

Acknowledgments: This work was produced within the scope of a master's thesis study titled "Ankara Yenimahalle Demetevler bölgesinde yapıların hızlı sokak taraması yöntemiyle değerlendirilmesi" (In Turkish) (Investigation of buildings with rapid street survey in Ankara Yenimahalle Demetevler region rapid street survey).

Conflicts of Interest: The authors declare no conflicts of interest.

References

1. Ateş, E. Determination of Soil Properties by Using Multi-Channel Analysis Method Records of Microtremor, Earthquake and Surface Waves: A Sample Implementation from AFAD Campus. *Artvin Çoruh Univ. Nat. Hazards Appl. Res. Cent. J. Nat. Hazards Environ.* **2021**, *7*, 240–251. [CrossRef]
2. Karabıyıkoğlu, T.; Dikmen, Ü. Dynamic Properties of Soils in The Western Part of Ankara. *J. Disaster Risk* **2022**, *5*, 196–215. Available online: https://dergipark.org.tr/tr/download/article-file/2365415 (accessed on 1 November 2026). [CrossRef]
3. Felek, G. Ankara'nın Batısındaki Yerleşim Alanlarının Zemin Yapısal Özelliklerinin Jeofizik Yöntemler ile Belirlenmesi. Master's Thesis, Sakarya University Institute of Science and Technology, Sakarya, Türkiye, 2019. Available online: https://acikerisim.sakarya.edu.tr/yayin/2022392 (accessed on 1 November 2026).
4. Sucuoğlu, H.; ve Yazgan, U. Simple survey procedures for seismic risk assessment in urban building stocks. Seismic assessment and rehabilitation of existing buildings. *NATO Sci. Ser.* **2003**, *29*, 97–118. [CrossRef]
5. Valente, M. Seismic protection of R/C structures by a new dissipative bracing system. *Procedia Eng.* **2013**, *54*, 785–794. [CrossRef]
6. Valente, M. Seismic upgrading strategies for non-ductile plan-wise irregular R/C structures. *Procedia Eng.* **2013**, *54*, 539–553. Available online: https://www.sciencedirect.com/science/article/pii/S1877705813004037 (accessed on 1 November 2026). [CrossRef]
7. Sucuoglu, H.; Yazgan, U.; Yakut, A. A screening procedure for seismic risk assessment in urban building stocks. *Earthq. Spectra* **2007**, *23*, 441–458. [CrossRef]
8. Yakut, A.; Sucuoğlu, H.; Akkar, S. Seismic risk prioritization of residential buildings in Istanbul. *Earthq. Eng. Struct. Dyn.* **2012**, *41*, 1533–1547. [CrossRef]
9. Sonmezer, Y.B.; Bas, S.; Akbas, S.O. Seismic risk estimation of the Kirikkale province through street survey based rapid assessment method (SSRA). *Earthq. Struct.* **2018**, *14*, 615–626.
10. Yeniçelik, C. Ankara Çankaya Ilçesi Kuzey Kesimi Yapı Stokunun Hızlı Sokak Taraması Yöntemiyle Değerlendirilmesi. Master's Thesis, Kırıkkale University, Kırıkkale, Türkiye, 2022.
11. Aynur, S.; Meydanli Atalay, H. Comparative analysis of existing reinforced concrete buildings damaged at different levels during past earthquakes using rapid assessment methods. *Struct. Eng. Mech.* **2023**, *85*, 793–808.
12. Harirchian, E.; Aghakouchaki Hosseini, S.E.; Jadhav, K.; Kumari, V.; Rasulzade, S.; Isık, E.; Wasif, M.; Lahmer, T. A review on application of soft computing techniques for the rapid visual safety evaluation and damage classification of existing buildings. *J. Build. Eng.* **2021**, *43*, 102536. [CrossRef]
13. Kassem, M.M.; Beddu, S.; Ooi, J.H.; Tan, C.G.; Nazri, F.M. Assessment of seismic building vulnerability using rapid visual screening method through web-based application for Malaysia. *Buildings* **2021**, *11*, 485. [CrossRef]
14. Nanda, R.P.; Damarla, R.; Nayak, K.A. Android application of rapid visual screening for buildings in Indian context. *Structures* **2022**, *46*, 1823–1836. [CrossRef]
15. Park, M.; Ju, Y.K. Disaster assessment of tall buildings in Korea by K-Rapid Visual Screening system focusing on structural safety. *Buildings* **2022**, *12*, 442. [CrossRef]
16. Purushothama, C.; Monteiro, R. Evaluation of rapid visual screening assessment of existing buildings using nonlinear numerical analysis. *J. Build. Eng.* **2023**, *76*, 107110. [CrossRef]
17. Mangir, A.; Okumus, V. Pre-earthquake fuzzy logic-based rapid hazard assessment of reinforced concrete buildings. *Case Stud. Constr. Mater.* **2023**, *19*, e02534. [CrossRef]
18. Bektaş, N.; Kegyes-Brassai, O. Enhancing seismic assessment and risk management of buildings: A neural network-based rapid visual screening method development. *Eng. Struct.* **2024**, *304*, 117606. [CrossRef]
19. Grover, R.K. Seismic vulnerability assessment of buildings using rapid visual screening for hybrid UMNN-RFO approach. *Int. J. Constr. Manag.* **2024**, *25*, 1177–1185. [CrossRef]
20. Mulwa, J.K. Systematic Seismic Events Discrimination Methods at the Kenya National Data Centre (N090). *Pure Appl. Geophys.* **2024**, *182*, 4867–4877. [CrossRef]
21. Zymvragakıs, A.; Javırıs, G.; Kouskouna, V.; Voulgarıs, N. Probabilistic Seismic Hazard Assessment for Boeotia (Central Greece) Utilizing a Complex Logic Tree Approach. *Pure Appl. Geophys.* **2025**, *182*, 3537–3552. [CrossRef]
22. Hamdache, M.; Peláez, J.A.; Henares, J. Contribution to Probabilistic Seismic Hazard Assessment and Its Uncertainty for Northeastern Algeria. *Pure Appl. Geophys.* **2025**, *182*, 439–471. [CrossRef]

23. Salim, M.R.; Yazdani, A. Estimation of Hazard-Dominating Scenario in Seismic Demand Analysis. *Pure Appl. Geophys.* **2025**, *182*, 473–489. [CrossRef]
24. Yan, Y.; Feng, J.; Li, G.; He, J.; Ma, T.; Feng, L.; Wu, M.; Zhang, B.; Zhou, Z. A hybrid CNN-LSTM method for seismic classification and time-series response prediction of disconnect switch. *Buildings* **2026**, *16*, 2131. [CrossRef]
25. Chen, C.S. Data-driven preliminary seismic evaluation of school gymnasiums: An integrated framework of artificial intelligence and multivariate statistical analysis. *Buildings* **2026**, *16*, 2909. [CrossRef]
26. Harirchian, E.; Lahmer, T.; Buddhiraju, S.; Mohammad, K.; Mosavi, A. Earthquake safety assessment of buildings through rapid visual screening. *Buildings* **2020**, *10*, 51. [CrossRef]
27. Bıçakcı, C.; Karataş, K.; Yıldız, S.S.; Bilgilioğlu, S.S.; Karaman, H. Explainable ensemble learning for rapid seismic damage assessment: A comprehensive benchmark using real data from the 2023 Kahramanmaraş earthquakes. *Buildings* **2026**, *16*, 2660. [CrossRef]
28. Rodrigues, P.Q.; Pantoja, J.C.; Varum, H. Reliability-based seismic safety assessment of the Metropolitan Cathedral of Brasília. *Buildings* **2024**, *14*, 1916. [CrossRef]
29. Rodrigues, P.Q.; Pantoja, J.C.; Varum, H. SeismicV: A mobile tool for assessing the seismic vulnerability of buildings. *Buildings* **2025**, *15*, 2541. [CrossRef]
30. Yenimahalle Belediyesi. Yenimahalle Hakkında. 20 August 2026. Available online: https://www.yenimahalle.bel.tr/Icerik/yenimahalle-hakkinda/3 (accessed on 20 August 2026).
31. Afet Riski Altındaki Alanların Dönüştürülmesi Hakkında Kanun [Law on the Transformation of Areas under Disaster Risk], No. 6306. *Official Gazette*, No. 28309. 2012. Available online: https://www.mevzuat.gov.tr/mevzuat?MevzuatNo=6306&MevzuatTur=1&MevzuatTertip=5 (accessed on 1 November 2026).
32. AFAD. *Türkiye Deprem Tehlike Haritası* [Turkey Earthquake Hazard Map]. Afet ve Acil Durum Yönetimi Başkanlığı. 2018. Available online: https://www.afad.gov.tr/turkiye-deprem-tehlike-haritasi (accessed on 1 November 2026).
33. T.C. Çevre ve Şehircilik Bakanlığı. *Riskli Yapıların Tespit Edilmesine İlişkin Esaslar* [Principles Regarding the Detection of Risky Buildings]. 2019. Available online: https://webdosya.csb.gov.tr/db/altyapi/icerikler/r-skl–yapilarin-tesp-t-ed-lmes-ne-il-sk-n-esaslar-20190218134628.pdf (accessed on 1 November 2026).
34. Bakırcı Er, Ş.; Eser, R.S. Investigation of Buildings with Rapid Street Survey in Ankara Yenimahalle Demetevler Region. In *Proceedings of the International Korkut Ata Scientific Researches Conference*; Osmaniye Korkut Ata University: Osmaniye, Türkiye, 2022.
35. *TS 500*; Requirements for Design and Construction of Reinforced Concrete Structures. Turkish Standards Institution: Ankara, Türkiye, 2000.
36. *TBDY 2018*; Turkish Building Earthquake Code. Ministry of Environment, Urbanisation and Climate Change: Ankara, Türkiye, 2018.

Disclaimer/Publisher's Note: The statements, opinions and data contained in all publications are solely those of the individual author(s) and contributor(s) and not of MDPI and/or the editor(s). MDPI and/or the editor(s) disclaim responsibility for any injury to people or property resulting from any ideas, methods, instructions or products referred to in the content.